Development of Electrosynthetic methods for the functionalisation of tertiary amides

Mandeep Kaur

September 2016

A thesis submitted in fulfilment of the requirements of the Manchester Metropolitan University for the degree of Master of Science by Research.

School of Science and the Environment

Faculty of Science and Engineering

Manchester Metropolitan University

Acknowledgements

First and foremost, I would like to express my appreciation and gratitude to my director of studies Dr. Alan M. Jones, for allowing me to undertake this project and guiding me throughout. I would also like to thank Professor Craig E. Banks for his advice throughout the project. I am also thankful to Dr. Chris W. Foster and Dr Elena Bernalte for their continuous advice and support during this project.

Last but not the least to my friends and family for their continuous support.

Abstract

Electrosynthesis is the formation of an organic molecule through the application of a potential across the surface of an electrode. There are numerous factors that make electrosynthesis an appealing method of synthesising and manipulating organic compounds, these include the ability to carry out a reaction at room temperature without additional chemical reagents. Importantly, electrosynthesis is considered one of the green chemistry technologies of the future.

The aim of this project is to investigate how electrosynthesis can be applied and understood in the functionalisation of amides using the Shono-type oxidation. Amides are abundant in nature, and are of importance to the development of pharmaceuticals, being present in biological systems such as proteins and peptides.

This thesis explores at how to generate a new C-X bond from a C-H bond (where X can be carbon or a heteroatom) adjacent to the nitrogen of an amide or carbamate by using "traceless electrons". C-H bonds are inherently unreactive and this method, when fully understood, will be a powerful way to selectively functionalise organic molecules.

To achieve this goal, new electrode materials have been investigated including the characterisation of reticulated vitreous carbon electrodes and pencil drawn electrodes in electrosynthesis. Several techniques have been employed such as cyclic voltammetry and scanning electron microscopy to understand the electroanalytical properties and characterisation of the electrodes. Both galvanostatic and potentiostatic methods will be used for the electrosynthetic C-H activation of the amides using a selection of electrolytes and conditions.

The sustainable electrosynthetic functionalisation of these fundamental organic molecules will enable the chemistry community to apply electrosynthesis more widely.

Abbreviations

Abbreviation	Definition
RVC	Reticulated vitreous carbon
PPI	Pores per inch
HET	Heterogeneous transfer rate
SEM	Scanning electron microscopy
PDEs	Pencil Drawn electrodes
SPEs	Screen Printed electrodes
mA	Milliamps
A	Amps
TBAP	Tetrabutylammonium perchlorate
E	Electrochemical reaction
C	Chemical reaction

Table of Contents

Table of Figures

Table of Tables

Table of Scheme

Chapter 1 – Introduction

Electrosynthesis is an emerging area within sustainable organic chemistry that can potentially accomplish the multiple criteria needed to develop more environmentally-friendly processes for the preparation of organic molecules.[1] These include the ability to monitor, the electrochemical process in real-time, giving rapid feedback on the chemical reaction as it happens, improving energy efficiency (reaction takes place at room temperature and no involvement of chemical "middle men", the electron is the reagent) and reducing the waste produced (atom economy) compared to traditional chemical methods.[1]

Several technologies have had a renaissance recently such as mechanochemstry[2] (reactions induced by the input of mechanical energy, such as grinding) biocatalysis,[3] photochemistry[4] and electrochemistry [5-9] in the field of synthetic organic chemistry, that are not only regarded "green chemistry" but are also more efficient and have favourable atom economy.[10-12]

Early examples of preparative electrochemistry can be found in the late 19th century where it was employed in industrial processes such as the chloralkali process [13] where chlorine gas and sodium hydroxide are produced when brine is electrolysed. Another example is the production of elemental aluminium by electrolysis of molten Al_2O_3 known as Hall−Héroult process.[13] These electrochemical methods are still in use in the 21st century producing millions of metric tonnes of these valuable chemicals.[14]

Despite the use of electrochemistry on an industrial level, [15] there is a lack of examples of using electrochemistry in organic synthesis and the fine chemicals industry. When compared to using traditional chemistry, electrosynthesis uses relatively mild conditions, has good functional group tolerance and high chemoselectivity.[14] Some synthetic chemists may be hesitant to adopt this technology into their research due to fears that product separation is difficult, and only aqueous solvents may be employed.[14] The reaction setup is perceived to be complicated (divided/undivided cell, potentiostat/galvanostat) and a number of reaction variables to control (electrolyte, electrode composition, cell type) and finally the cost associated with buying additional instruments.[14] Although electrochemistry is slowly being adapted into research,[16,17,18] however, there is no standard

instrumentation for preparative electrolysis, and there is a trend in recent literature for using homebuilt rather than commercially available equipment.[14,19] This intriguing area of chemistry is still in its infancy when it comes to a fundamental understanding of the underlying parameters and will be the subject of this study.[16] Amides have been selected as they are present in fundamental building blocks and play a major role in synthesis of pharmaceuticals, agrochemicals and polymers.[20] Amides are a key functional group in organic chemistry[21] and are crucial in the elaboration and composition of biological and chemical systems. Numerous bioactive products also have prevalent amide bond linkage.[22]

1.2 What is electrosynthesis?

Electrosynthesis is the formation of an organic molecule through the application of a potential across the surface of an electrode.[1,23-24]

A_{ox}= Oxidised substrate; A_{red}= Reduced substrate; X= Halogen;
Nu= Nucleophile; E= Electrophile
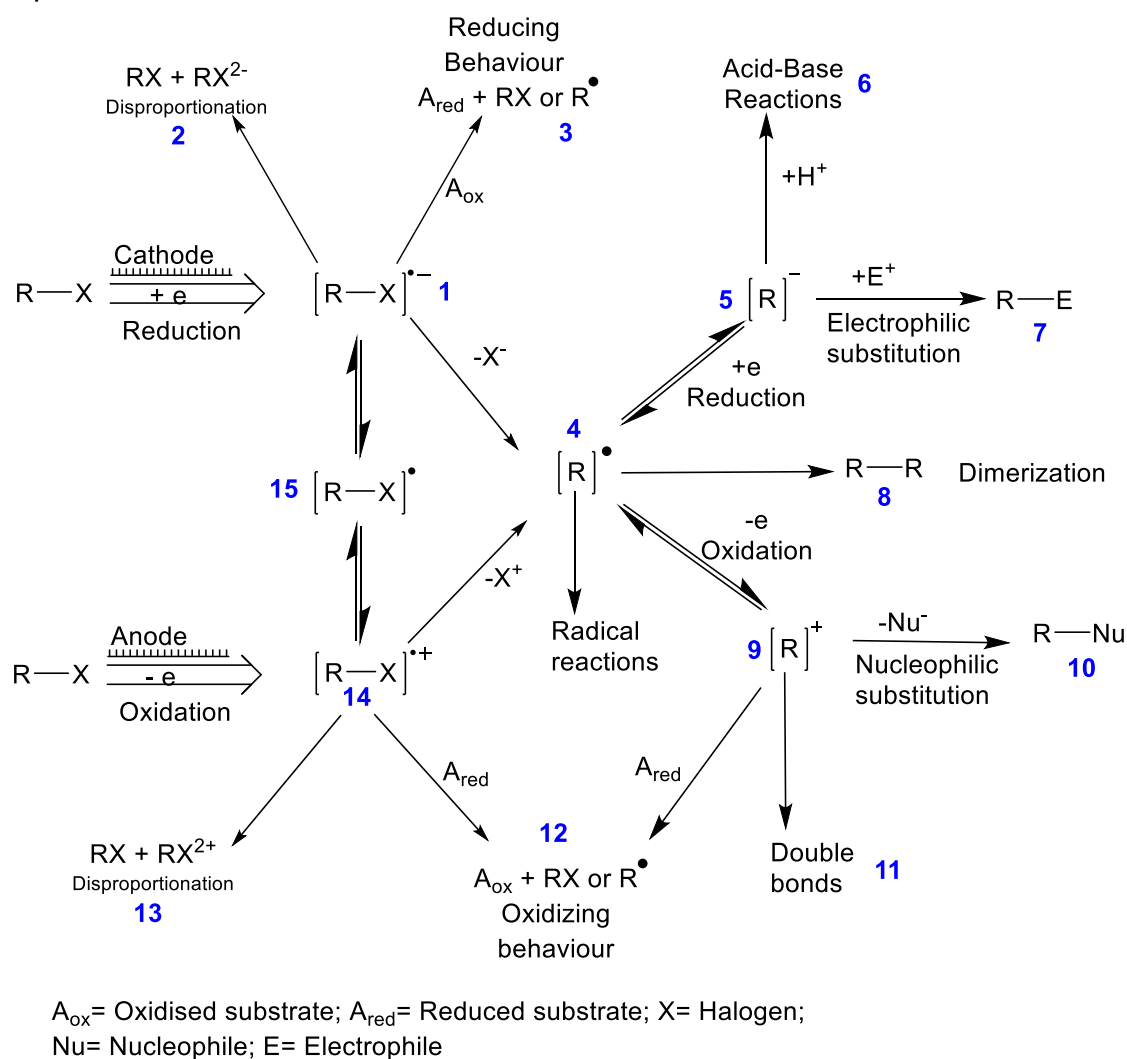
Figure 1.2.1: Potential reactive intermediates formed electrochemically and subsequent chemical reactions that afford the final products during an electrosynthetic reaction.[25]

Figure 1.2.1 shows several mechanistic pathways a reaction can take; at cathode or anode, neutral organic compounds are reduced to radical anion (**1**) or radical cation (**14**). Radical anion (**1**) is oxidised to form disproportionation (**2**) and neutral compound or a radical and a reduced substrate (**3**). The radical anion and cation lose halogen group and form a radical (**4**). (**4**) oxidises further to anion (**5**) or cation (**9**). Removal of hydrogen ion from (**5**) leads to acid-base reaction (**6**) and electrophilic substituted leads to a neutrally substituted compound (**7**). (**4**) also leads to formation of dimerization (**8**). Cation (**9**) undergoes nucleophilic substituted to form a neutral substituted compound (**10**) and can lead to formation of double bonds (**11**). (**14**) is reduced to form an oxidised substrate and neutral compound or a radical (**12**). Reduction of a compound occurs when a molecule's LUMO (lowest unoccupied molecular orbital) gains an electron from the cathode. Similarly, oxidation is triggered at the anode when an electron is removed from the HOMO (highest occupied molecular orbital).[1]

Electrochemical reactions of organic compounds are a combination of two processes. A reactive intermediate (radical-cation or radical-anion) is formed when the electrochemical process with the molecule (heterogeneous electron transfer) takes place at the electrode surface (E) and the chemical process (C) that occurs in solution. The combination of these two processes chemical (C) and electrochemical (E) can be repeated to allow diverse kinetic sequence, e.g.: EE, EC, ECE. Figure 1.2.1[25] demonstrates possible reactive intermediates formed. Something that is possible by using electrochemistry but is not easily achieved by traditional organic chemistry is an inversion of the reactivity of a functional group (*umpolung*)[26] which takes place when electron transfer occurs during the electrochemical process; electron-rich compounds become electron deficient when oxidised, and nucleophiles are converted to electrophiles. Furthermore, nucleophilic reactive sites are formed when reduction converts electron-deficient centres to electron-rich centres. This feature of electrochemistry makes it a powerful strategy for the synthesis of complex molecules (see section 1.5)   and hence may lead to synthetic routes in the future that diverges from those of classic organic chemistry.

1.4 Why is electrosynthesis green methodology?

Electrosynthesis is considered "green chemistry" as generating organic compounds electrochemically makes it less polluting than conventional methods as the electrons are the reagents.[15] Listed below are advantages of using electrosynthesis to perform reactions:

1. Most electrosynthetic reactions occur at room temperature. Hence the energy of the electrons can be controlled by the applied voltage.[25]

2. Atom economy can be improved significantly as there is a possibility to perform direct or indirect reactions and paired electrolysis (when simultaneously electrochemical reaction takes place at both working and counter electrode, both electrodes are considered working electrodes).

3. Current density or applied potential can be adjusted to control reaction rates.[27]

4. Electroanalytical techniques (cyclic voltammetry) can assist in electrosynthetic experimental conditions and pathway.[25]

5. The electrons are clean reactants electrons are used as reagents.

6. Electrosynthesis of chemical products [15, 28-29] would lead to the use of fewer chemicals in a processes.

7. When compared to classical chemical analyses, the costs associated with the reactions are minimised as reactions can be monitored in real-time and provide feedback on the chemistry taking place during the chemical process.

As with every method, there are few disadvantages associated with electrochemistry. However, there are possible solutions to these problems:

1. Heterogeneous reactions are slower than homogeneous reactions as they occur at the electrodes and take place at the interface between an electrolyte and electrode (limited in area and movement). However, this can be improved by using high surface area electrodes to offer larger mass-transport parameters.[25]

2. There are technical difficulties and cost associated with recovering the supporting electrolyte. Again this can be minimised with the aid of micro flow cells, which have a very small distance between the electrodes.[30-32] This technique not only enhances the rate of chemical reaction that follows the

electron transfer but also increases the mass transport.[31-33] Thus lowering concentrations of the supporting electrolyte required for the reaction.

3. Using cells divided by a separator leads to a higher resistance to charge transport. However, the separator can be omitted if sacrificial anodes are used. Alternatively, conductive membranes of low resistance can be employed (*e. g.* , NafionTM).

1.5 Current research in electrosynthesis

Although the electrosynthesis of complex molecules is scarce in the literature, nonetheless selected examples in this section will be used to illustrate the power of electrochemical transformation and its complexity-generating power. In the past 20 years, Moeller[34-36] and Wright's[37-38] groups have demonstrated significant advances in electrochemical oxidative coupling reactions.

Harran *et. al* [18] demonstrated that the synthesis of DZ-238 (a diazonamide-inspired preclinical candidate for oncology) (Figure 1.5.1) can be scaled up by an electrochemical reaction and hence showcased the remarkable functional group compatibility.[18] It should be noted that to make same compound previously oxidants such as PhI(OAc)$_2$ [39] was required leading to considerable by-products formed and produced an inactive diastereoisomer. However, when electrochemical conditions were applied, it improved not only the selectivity but also the cost and the environmental footprint enabling the reaction to be easily carried out on a larger scale.[14]
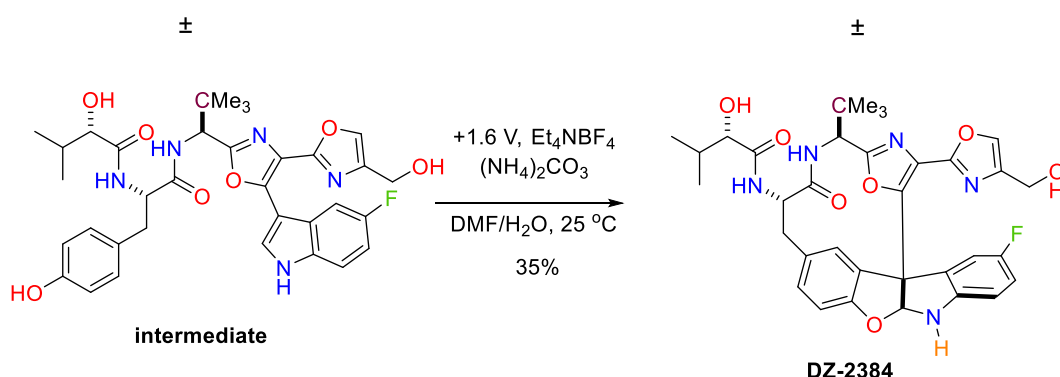
Scheme 1.5.1: Synthesis of DZ-238(diazonamide-inspired) by Harran and co-worker.[19]

Reduction of a geminal dihalide (Figure 1.5.2) electrochemically was demonstrated by a collaboration between Waldvogel group and Novartis.[40] Previous reaction using traditional route (birch reduction or hydrogenolysis) led to ring-opened products and racemization. The group also tried electrochemical dehalogenations, however using this method required lead or mercury cathode which are unsuitable for pharmaceutical materials. To circumvent these issues electrosynthesis was achieved by using a separated cell and leaded bronze cathode as electrode and [Et$_3$NMe]O$_3$SOMe as electrolyte. They demonstrated that this modified electrochemical method can not only lead to significantly less waste and higher cost-efficiency but also fixed the problems related to racemization and ring-opening.[40]
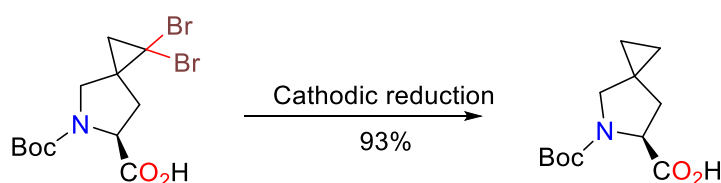
Scheme 1.5.2: Synthesis of NS5A (protein) inhibitor intermediate.[40]

Baran[17] *et. al* published the use of electrochemical oxidation to prepare a complex natural product, (Dixiamycin B) (Figure 1.5.3). Accessing the dimeric natural product dixiamycin B proved difficult and no suitable reagent-based oxidant was efficient enough to forge the necessary N-N bond required, therefore electrochemical oxidation was used.[17] The electrochemical reaction was performed by treating a carbazole using a potentiostatic method (constant potential of 1.15 V is applied), tetralkylammonium bromide electrolytic solution and graphite rod as electrodes leading to the formation of dixiamycin B and thus showcased the remarkable functional group compatibility achieved by using electrosynthesis.
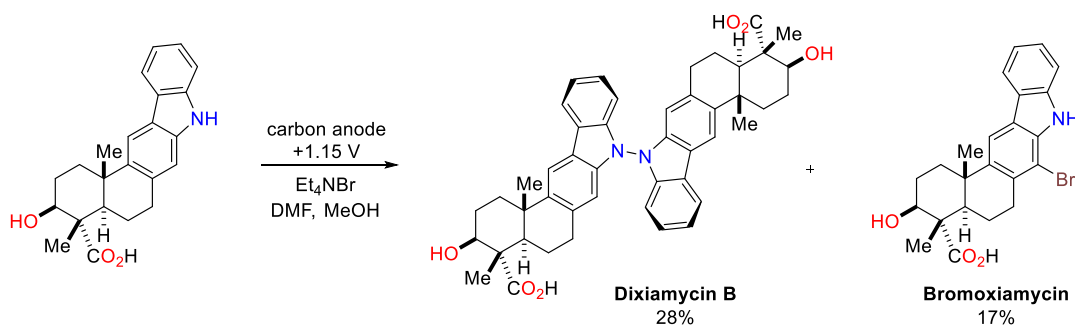
Scheme 1.5.3: Synthesis of dixiamycin B by Baran and co-workers.[17]

Moeller and colleagues recently applied electrochemical oxidation and reduction reactions to show oxidation of veratryl alcohol to the corresponding aldehyde at the anode (Scheme 1.5.4).[41] The success of this paired electrolyses illustrated how oxidation reactions of syringealdehyde could be improved. The group selected syringealdehyde because they are better partner for paired valorisation and because oxidative condensation converts the aldehyde into a new molecule not typically associated with lignin. [42] Before the paired electrochemical reactions for the valorisation of lignin derived materials could be considered, there were several parameters that had to be modified for the syringealdehyde reaction such as the current used, the mediator, the solvent ratios, the concentration of the electrolyte and carrying out electrochemical reaction in divided or undived cell. Undivided cells were selected as there is no chance of the radical cation being reduced back to starting material and increased electrolyte concentration (0.1 M to 0.5) improved conversion of the reaction. The final selected solvent ratios, and the current selected are shown in scheme 1.5.5.[42]

Reticulated vitreous carbon was used as electrode (see Chapter 2 for further details).[42] Several steps and reaction conditions were tested (number of F/mole, current, mediator) before a sufficient yield of the end product was achieved. Better control of the intermediate was required in order to utilise the paired electrolysis in the future, even though the reaction benefited from the optimised conditions.
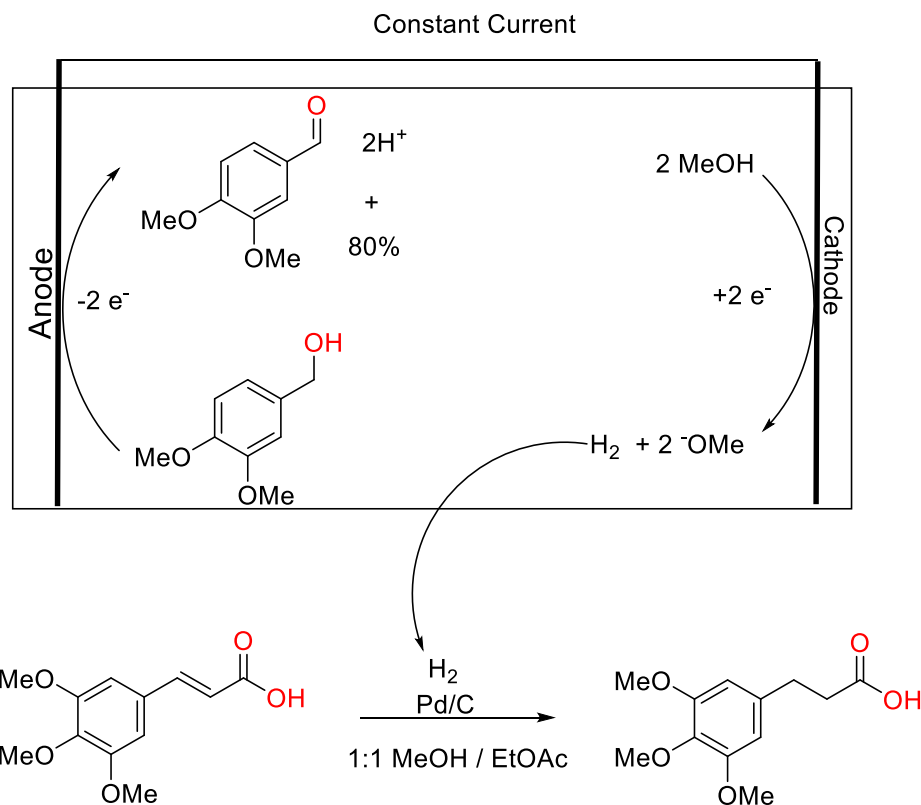
Scheme 1.5.4 A paired electrolysis for the processing of lignin derived materials.[41]
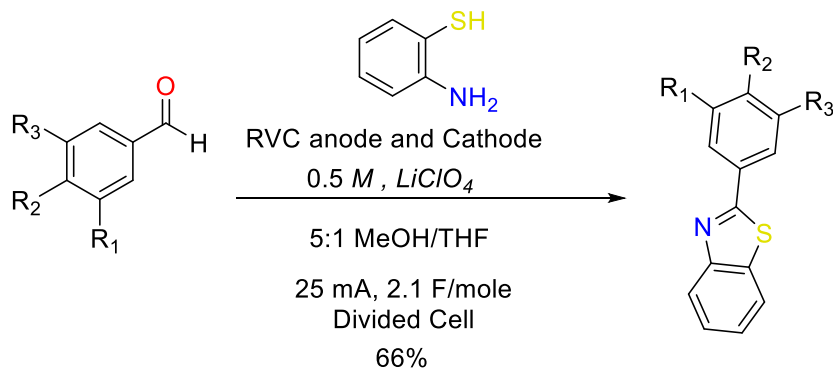
Scheme 1.5.5: Optimised divided cell reaction.[42]

Traditional methods that exist for C_{sp}^3-H/aromatic C-H cross-coupling for connecting an aliphatic part and an aromatic part in synthesis of complex organic molecules such as transition-metal-catalysed activation of C_{sp}^3−H bonds, Minisci-type reactions and Friedel−Crafts-type reactions.[43] However, these types of reactions lead to over- reaction, to overcome these Yoshida *et al.* investigated several electrochemistry methods scheme 1.5.6a shows C_{sp}^3-H/C_{sp}^3-H cross coupling reaction by electrochemical oxidation.[43] Unfortunately, these C_{sp}^3-H/aromatic C-H cross coupling suffer from overoxidation because the cross-coupling products,

alkylated aromatics, usually have lower oxidation potentials than the starting materials. Scheme 1.5.6 although overoxidation is not a problem with cation pool method. It cannot be applied to benzylic cations, which are too unstable to be accumulated in solution even at low temperatures.[43] To overcome the problems in these reactions Yoshida *et. al*[43] screened several stabilising agents (sulfilimines were selected as stabilising agents) to be utilised in electrochemical reactions. Scheme 1.5.6c demonstrates C−H/aromatic C−H cross-coupling achieved by the electrochemical generation and accumulation of stabilized benzyl cations followed by their reactions with subsequently added aromatic nucleophiles. They demonstrated that by using electrochemistry it is possible to generate organic cations in solutions in the absence of nucleophiles at low temperatures.[43] Electrochemical oxidation serves as a powerful method for generating reactive cationic species via C−H bond cleavage.
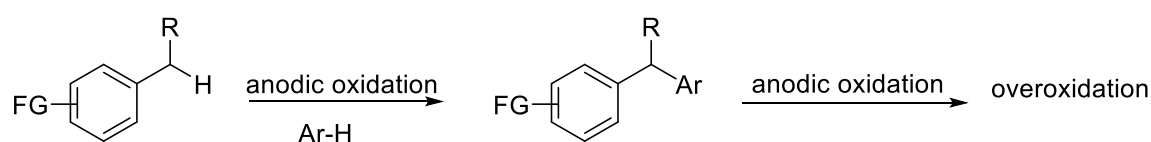
a. anodic oxidation in the presence of carbon nucleophiles
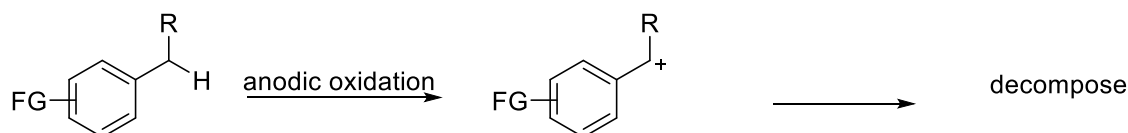
b. anodic oxidation in the presence of carbon nucleophiles(the cation pool method)
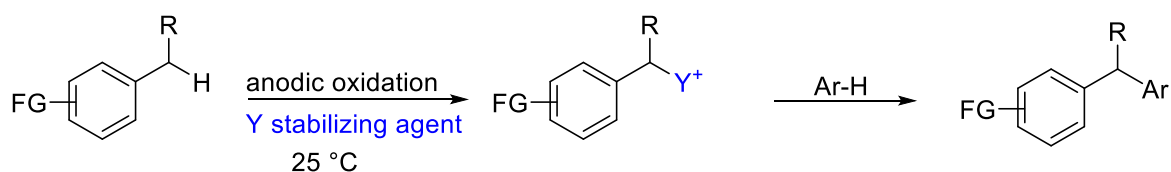
c. Yoshida's work using electrochemistry to produce cation and stabilixing agent.

Scheme 1.5.6: Three approaches to electrochemical Benzylic C-H/Aromatic C-H cross coupling.[43]

Baran *et al.* [44] also demonstrated the electrochemical allylic C-H oxidation and gave examples of over 40 synthesised compounds.[44] They used an inexpensive graphite plate electrode and $LiBF_4$ as the electrolyte. When similar reactions are carried out without electrochemistry, toxic waste (using reagents based on chromium or

selenium)[45] is produced and have less energy efficiency. The group explored several criteria's that lead to identification of conditions (modification included co-oxidant, new electrochemical mediator, design of set-up etc.) needed to perform a synthetically useful electrochemical allylic C-H oxidation.[44]
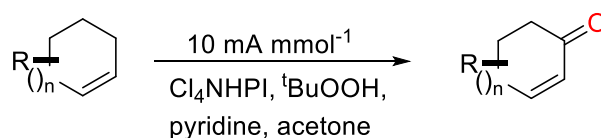
Figure 1.5.7: Electrochemical allylic C-H oxidation.[44]

Inspired by the recent advances being made in electrochemistry, we decided to investigate the anodic oxidation of amides using Shono oxidation. The next subsection will briefly explain what Shono oxidation is and why is it important.

1.6 Shono-Oxidation

The first direct electrochemical anodic oxidation of α-methylene group to tertiary amide or carbamate was reported by Shono and colleagues [46] (Figure 1.6.1).[47] This generated a new carbon-carbon bond *via* an anodic methoxylation step, Lewis acid mediated generation of an *N*-acyliminium ion intermediate which was intercepted with a carbon-based nucleophile (e.g. Grignard reagent).[48] Using this approach the C-H group adjacent to the amide can be transformed to C-X bonds (e.g. C-C, C-O, C-N, C-S, C-P etc.) [16]. Shono oxidation has been extensively reviewed by by Yosida [48] and Jones and Banks.[49]
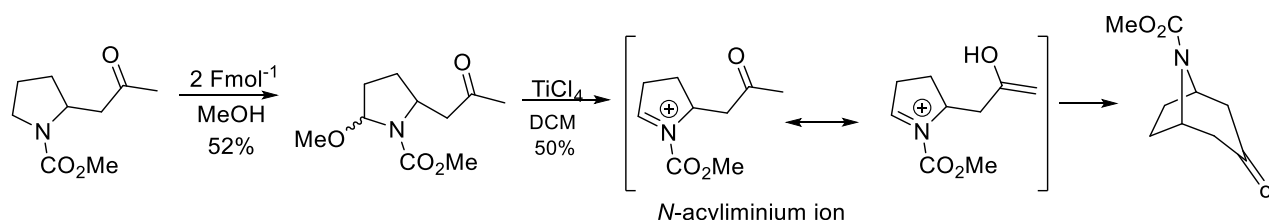
Scheme 1.6.1. Generation of new carbon-carbon bonds via anodic application.[47]

Shono-Flow electrochemistry (Figure 1.6.2) was utilised by Ley and co-workers[50] where they synthesised the indole alkaloid natural product nazlinine. Initially, they utilised steel or platinum-coated electrodes in conjunction with equal amount of

tetraethylammonium tetrafluoroborate as electrolyte, however it was observed that no conversion of the product was occurring. Therefore, they changed the electrode to carbon anode resulting in the desired reaction.[50]
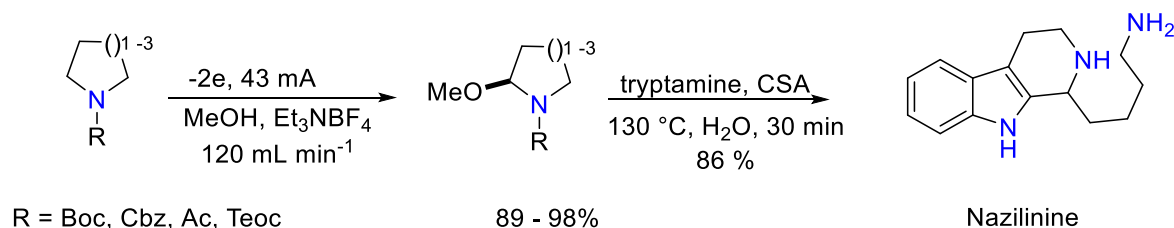
Scheme 1.6.2: Shono flow electrochemistry for two-step preparation of nazlinine.[50]

The Shono oxidation has not been systematically investigated. However, the Jones and Banks groups have carried out preliminary investigations into the Shono oxidation.[16] Suárez *et al.*[16] investigated the cyclic voltammetry behaviour of amides (Scheme 1.6.3) they explored numerous parameters such as how optimisation of the applied voltage results in selective oxidation.[16] The choice of electrolyte and its effect on the outcome of reaction and the conversion rate with varying charge; at a constant voltage were also investigated. It was found that TBAP was a suitable electrolyte, charges between 1.7 V and 2.0 V gave the optimum conversion.[16] Tertiary amide undergoes a single electron oxidisation at the working electrode forming a radical cation intermediate. The loss of a proton at α-position and another electron forms α-aminium ion, this aminium ion undergoes a nucleophilic attack from the solvent (methanol) losing a proton to form an a-methoxy amide, this is the Shono-oxidation.
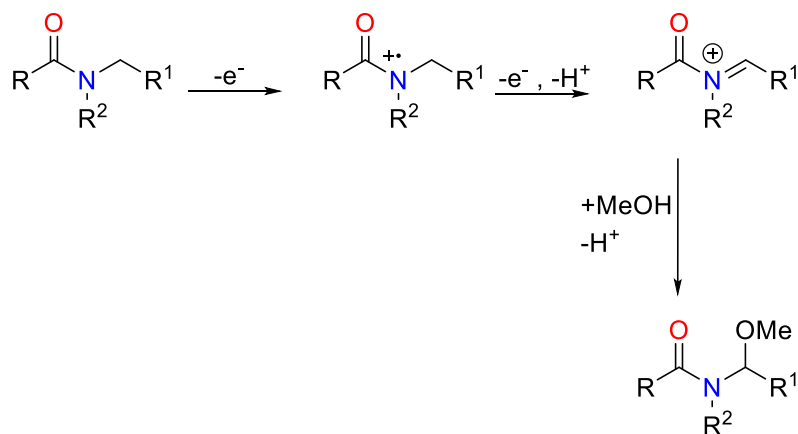
Scheme 1.6.3: A possible mechanism for the Shono oxidation by Suárez *et al[16]* where X can be C-O, C-S, C-C or C-N.[16]

1.9 Aim

Electrosynthesis is an upcoming area which offers an alternative for synthesising complex and natural compounds, it can also be implemented into existing techniques. It is considered "green" as it reduces the by-products and the reactions can be carried out at the room temperature. The chapters in this thesis will provide information about the electrode material (RVC) when applied in electrosynthesis. Exploring how electrodes fabricated in the lab can be utilised for electrosynthesis and also for electroanalytical method. How cyclic voltammetric (CV) scan rate study of the organic compounds can provide information on the oxidation potential. The electrosynthesis of the compounds is conducted by holding the reaction at the chosen potential. Chapter 5 will compare how potentiostatic and galvanostatic methods. The overall goal of this research is to contribute a greater understanding on the electrosynthesis of tertiary amide and the electrosynthetic parameters for the benefit of scientific community, as well as understanding the parameters of the Shono oxidation.

Chapter 2 – Reticulated Vitreous Carbon

2.1 Introduction

Reticulated Vitreous Carbon (RVC) electrodes were selected to be used in the Shono oxidation of amides (Scheme 1.6.3) and will be characterised and analysed in this chapter. Shono oxidation has not been carried out with the RVCs used for characterisation.

Initial electrochemical analysis check (CV to detect the oxidation potential) of the compound did not show any oxidation peaks therefore characterisation of RVC1 foam (as the working electrode) was required to check if the foam was defective. RVC2 and RVC3 were selected to compare the electrochemical responses. Shono oxidation was not carried out with the electrodes, as they were not giving any response in the electroanalytical phase of the research. The characterisation of RVC was carried out to examine if the electrodes are viable material for our proposed Shono oxidation electrosynthesis and electroanalytical characterisation of the compounds.

RVC is composed entirely of vitreous carbon, a form of pure carbon, produced by the thermal decomposition of three dimensionally crosslinked polymer (i.e. polyurethane and phenolic resins).[51-52] Compared to a common carbon based electrode (i.e. glassy carbon electrode), RVC has an exceptionally high void volume due to an open-pore foam material of honeycomb structure, which gives the material high surface area, rigid structure and low resistance to fluid flow.[53] In non-oxidising environments it can withstand high resistance to temperatures.[53] High rates of mass transport of the electroactive species to the electrode surface and uniform current throughout the experimental is achievable when using RVC as an electrode.[53] The principles of other carbon based material together with RVC as three dimensional electrodes have been reviewed in the literature.[54] In-general properties of vitreous carbon include low density, high thermal and electrical conductivity and a high corrosion resistance.[53] RVC as an electrode is suitable for organic electrosynthesis as it is resistant to organic solvents and oxidising agents. Other properties that make it a useful electrode material is the low electrical/ fluid flow resistance and high current densities.[55] High temperature insulation, scaffolds for biological growth,

storage batteries and synthesis of organics are some of the other applications of RVC. [56-60] Several electrodes pores per inch (PPI) of RVC have been investigated by Szanto et al. [61] for the electrosynthesis catecholamine and coumestan (Scheme 2.1). Electrochemical oxidation of catechol to orthoquinone forms a double Michael acceptor. The generated orthoquinone and 2-hydroxycoumarin leads to a double Michael addition type reaction followed by oxidation of the heterocycle to reform aromatic ring losing hydrogen gas. The reaction proceeds through an ECCE mechanism (where electrochemical (E), Chemical reaction(C)). Although the ability of RVC with PPI of 30, 60 and 100 were compared with that of a porous three-dimensional nickel electrode but no reaction conditions were given on synthesised products. The results revealed that 100 PPI RVC performed equally to the nickel stacked net but the performance of 30 and 60 PPI or significantly lower.
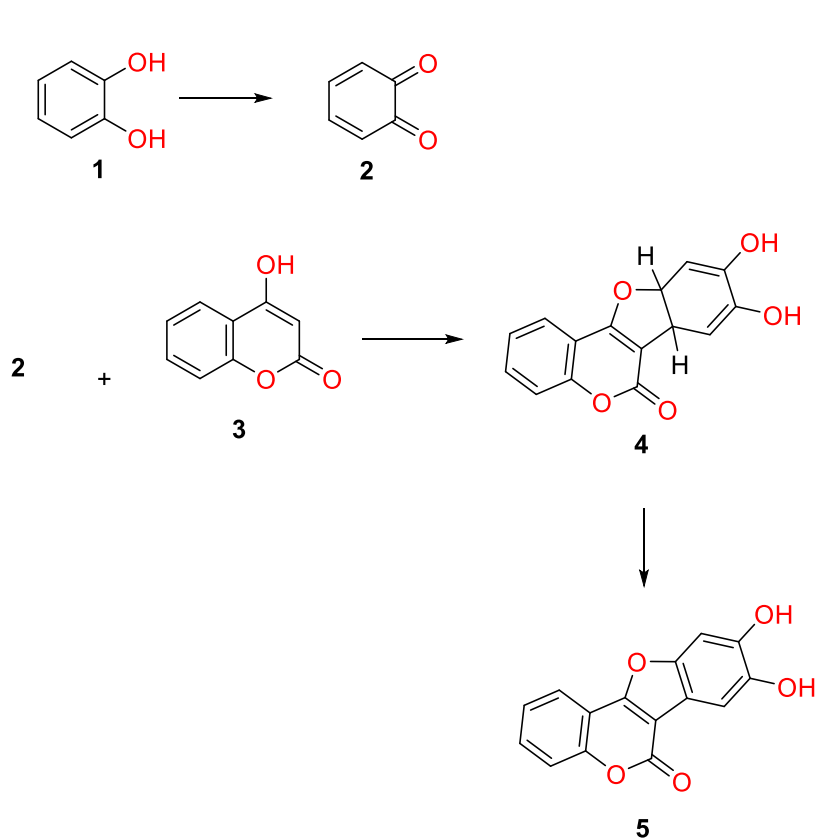
Scheme 2.1: Reaction scheme describing electrooxidation performed on Catechol (**1**), Orthoquione (**2**), 2-hydroxycoumarin (**3**), 1,6 dihydrocoumestan(**4**) and Coumestan (**5**).[61]

A review by Friedrich et al.[53] highlighted the current applications, where RVC is being implemented as an electrode material both in fundamental and applied electrochemistry. These include organic synthesis,[16,61] as sensors,[62] hydrogen peroxide production,[63] as batteries and fuel cells[64] and in metal ion removal. [65-66] Numerous advantages of using RVC as an electrode include the inertness and the stability of the electrodes when used in wide range of acids and bases. The stability of electrodes can be exploited in electrosynthesis to produce organic compounds[16,61] with better selectivity than other production routes when RVC is used as an electrode. Another property of RVC is the ability to withstand high temperature, as it does not combust after heating to a bright incandescence in air,[53] this is beneficial especially when cleaning the RVC to remove any solvents present in the electrode. However, RVC heated above 315 °C in air will produce a material with enhanced adsorption properties and would result in significant oxidation.[53] As with every electrode material there are downsides to using RVC as an electrode. The high void volume of the material makes it brittle which can break easily if not handled carefully. Metal and conductive organic coatings can modify RVC material. Other methods include impregnation with biochemical/organic/inorganic materials.[53] Inspired by the current research into the applicability of durable and low-cost RVC as electrodes. RVC will be used for the electrosynthesis in the project.

2.2 Electrochemistry Method

A typical electrosynthetic reaction contains two electrodes, an anode (positive pole connected to direct current power), cathode (negative pole) and a solution that contains salt (electrolyte), which improves conductivity of the solution by providing ions. The desired reaction takes place at the working electrode (WE). Electrons are removed from compounds that oxidise easily at the anode. These electrons are then transported through an electronic conductor (wire) to the power source and onto the cathode. The cathode is where another electrochemical reaction occurs and the electrons are transferred to the compound that is easily reduced. Occasionally divided cell (separate compartments) are employed to separate the electrodes, this is carried out to prevent reaction interference from products obtained at the individual electrodes such as to stop the oxidised material from being reduced again.

Electrosynthesis can be carried out either potentiostically or galvanostatically.[67] Potentiostatically, a 3 cell electrode setup (Figure 2.2.1), where the voltage is set,

and hence cyclic voltammetry (CV) of the compound is necessary to determine the oxidation potential. It should be noted that although the potential can be controlled the current will fluctuate as the resistance of the cell changes. Galvanostatically, a 2 cell electrode setup, is when only current is set, and therefore the oxidation potential of the compound does not need to be deduced. Although the galvanostatic method is operationally simpler it may lead to over-oxidation of the compound, as the voltage will fluctuate during the reaction.
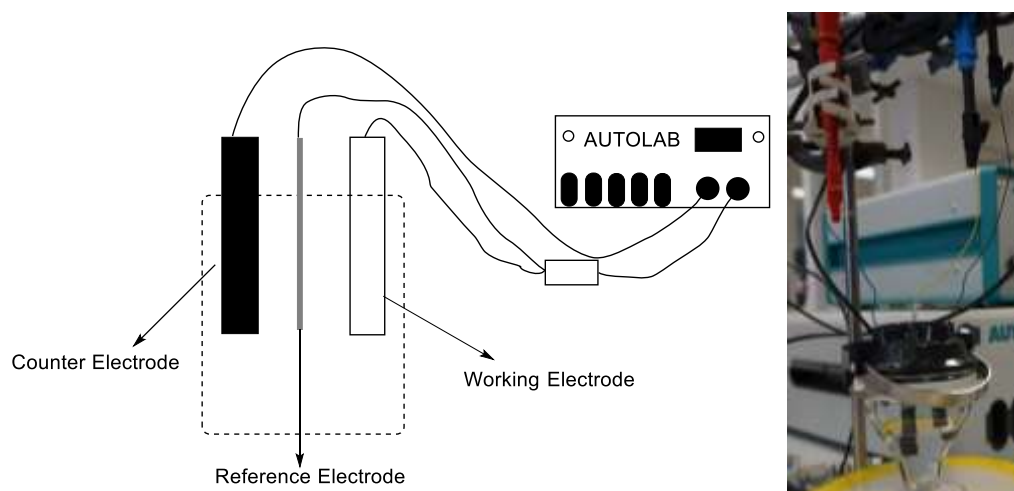
Figure 2.2.1: Typical 3 electrode set up used, working and counter electrodes are RVC and the reference is a silver wire.

2.3 Cyclic Voltammetry (CV)

Before potentiostatically-controlled electrosynthesis of a compound can be carried out the oxidation potential needs to be found. Therefore, an electroanalytical study is performed using cyclic voltammetry(CV) on the compound, at various scan rates.[68] Cyclic voltammetry is measuring the current that develops at the working electrode as a function of the applied potential and a plot of current versus potential is constructed (Figure 2.3.1).[67] Current increases with increasing scan rate and is dependent on the surface area of the electrode. The increase in current with scan rate is due to the diffusion layer and the time taken for a scan rate to complete. Lower scan rate experiments take longer to complete, and the diffusion layer will grow much further from the electrode when compared to a faster scan rate. There are several other factors that can affect the shape and size of the CV graph, such as conductivity of the electricity, although there is always conduction occurring during the experiment, oxidation and reduction peaks would not be visible if there is higher conductance occurring. Another factor that can effect CV is the resistivity

(opposition of the flow of electric current), higher resistivity would not display reduction peak. To calculate parameters related to the CV, Nicholson equation (2.4) is used, this gives information regarding the heterogeneous electron transfer rate k^0.
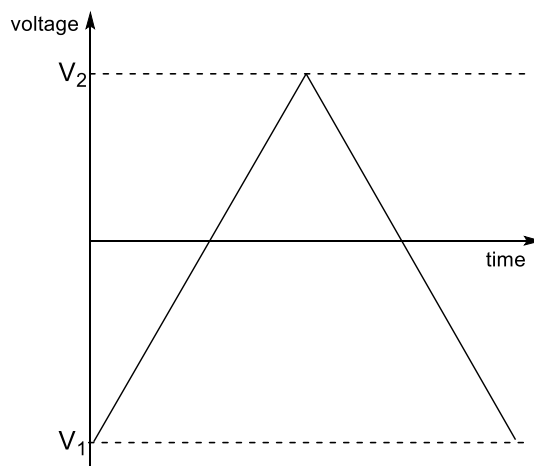
Figure 2.3.1: Cyclic voltammetry graph. The scan rate is reversed when the voltage reaches V_2 and the voltage sweeps back to V_1 the voltage is swept between two values at a fixed rate.[67]

2.4 Nicholson Method

The observed heterogeneous electron transfer rate k^0 is estimated routinely by using the Nicholson method. For quasi-reversible system; **Equation 1** is used:[69]

Equation 1:

$$\phi = k^0 \left[\frac{\pi D n v F}{(RT)} \right]^{-\frac{1}{2}}$$

The kinetic parameter is given by ϕ, diffusion coefficient of the electroactive species is D, number of electrons involved in the electrochemical process is n, Faraday constant (F), voltammetric scan rate (v), universal gas constant (R), and temperature of the solution (T).[70] For one-step, one electron process at a set temperature (298 K), the kinetic parameter, ϕ is tabulated as a function of peak-to-peak separation (ΔEP, mV).

An important factor to consider is ΔEP in terms of the performance of an electrode material and is used to determine the heterogeneous electron transfer rate(HET), where increased reversibility in the electrochemistry is represented by smaller ΔEP

at the redox probe utilised and thus faster HET kinetics at the given electrode material.[71] Equation 2 is the function of ɸ (ΔE_P), which fits Nicholson's data:[72]

Equation 2

$$\phi = \frac{(-0.0628 + 0.0021X)}{(1 - 0.017X)}$$

ΔE_P is represented by X in equation 2 and is used to determine ɸ as a function of ΔEP from the experimentally obtained voltammetry. From this, a plot of ɸ against $[\pi D n v F/(RT)]^{-\frac{1}{2}}$ can be produced graphically, allowing the standard heterogeneous rate transfer constant, k^0, to be readily determined. However, Equation 3 is used when ΔEP values exceed 212 mV within the Nicholson table:[73]

Equation 3:

$$k = \left[2.18\left(\frac{DanFv}{RT}\right)^{0.5}\right]\exp\left[-\left(\frac{(a^2nF)}{RT}\right)\times\Delta E_p\right]$$

α is the transfer coefficient and is assumed to correspond to 0.5. The k^0 values were calculated assuming diffusion coefficients of 9.10 × 10^{-6} for hexaammineruthenium(III) chloride and 9.00 × 10^{-6} for ammonium Iron(II) sulfate hexahydrate.[74,75] The rest of the constants stay the same as described in equation (1).

The equations above will be used to calculate the k^0 of the cyclic voltammetric analysis of the RVC electrodes and determining how fast or slow the electrodes are in measuring the electrochemical process or electron transfer properties.

2.5 Inner and Outer-sphere redox probe

The subsections below will briefly explain the difference between inner and outer sphere redox probe. These probe were selected to characterise the RVC as they are both different in chemical composition and specific compounds can be used to check the interaction of the functional groups on the surface of the RVC.

2.5.1 Outer Sphere Probe (OSP)

To characterise the interaction of RVC with outer-sphere electrochemical redox probe hexaammineruthenium(III) chloride ($Ru(NH_3)_6$ $^{3+/2+}$) (Scheme 2.5.1) will be used. The outer-sphere redox probe is only affected by the degree of edge plane sites/defects and the electronic structure of carbon based electrode materials. The probe is insensitive to the carbon/oxygen ratio groups.[76] On most graphitic electrodes, outer-sphere probe involves a straightforward electron transfer and therefore the electrode kinetics are relatively insensitive to the surface oxides/microstructure and adsorbed monolayers on sp^2 carbon electrodes.[77] The electron transfer does not rely upon interaction with functional group or surface site indicating that the rate of reaction is insensitive to surface modification.[77]

$$\left[Ru(NH_3)_6\right]^{2+} \rightleftharpoons \left[Ru(NH_3)_6\right]^{3+} + e^-$$
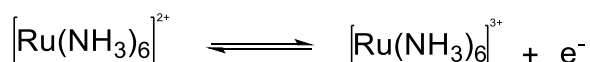
Figure 2.5.1: Oxidation of Hexaammineruthenium(III) chloride.

2.5.2 Inner Sphere probe (ISP)

To characterise the interactions of RVC with inner-sphere probe, ammonium iron (II) sulfate hexahydrate (Scheme 2.5.2) will be used. The probe is very sensitive to surface particularly to carbonyl groups but also to functional groups.[78,79] The following electrochemical responses are observed when inner-sphere redox probe is utilised by carbon based electrode material. Inner-sphere is influenced by the density of electronic states (DoS) near the Fermi level of the said material and more significantly by the surface microstructure, for example in terms of the presence of oxygenated species (which are either beneficial or detrimental) or the surface cleanliness.[80-81] The observed electron transfer processes are significantly accelerated with presence of edge plane like sites/defects present on the graphitic materials. Hence electrodes with large surface coverage of edge plane like sites would have an improved HET.[82] The content of oxygenated species comprising vitreous carbon electrode material and the electronic structure both play an important part in inner-sphere redox probe as the electrochemical response depends on both of these properties.[83]

$$[Fe]^{2+} \rightleftharpoons [Fe]^{3+} + e^-$$
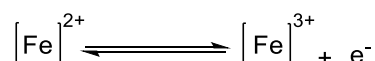
Figure 2.5.2: Reduction of Ammonium Iron(II) sulfate hexahydrate.
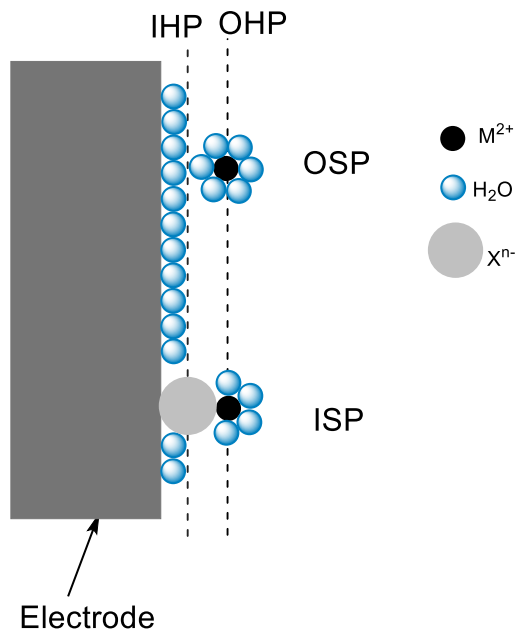
Figure 2.5.3: Inner sphere (ISP) and outer sphere (OSP) redox reaction paths at the electrode. X^{n-} is the ligand M^{2+} is the metal centre (Ruthenium). H_2O as soluble in water.[67]

Overall outer sphere has a weak interaction with the reactive species and is not sensitive to the structure.[67] Inner sphere processes proceed through common ligand shared by metallic centres and correspond to specifically adsorbed reactants. The reactant centre or ion of the outer sphere is in 'Outer Helmholtz Plane' and for the inner sphere it is in 'Inner Helmholtz Plane' (see Figure 2.5.3).[67]

2.6 Aim

The aim of electroanalytical study is to compare the RVC foam utilised in the electrochemistry for this project to the available RVC in the laboratory. To determine and compare the heterogeneous rate constant ($k^0\, cm\, s^{-1}$) of the RVCs. The overall goal is to determine the suitability and reasonable cost associated with the RVC selected.

2.7 Results
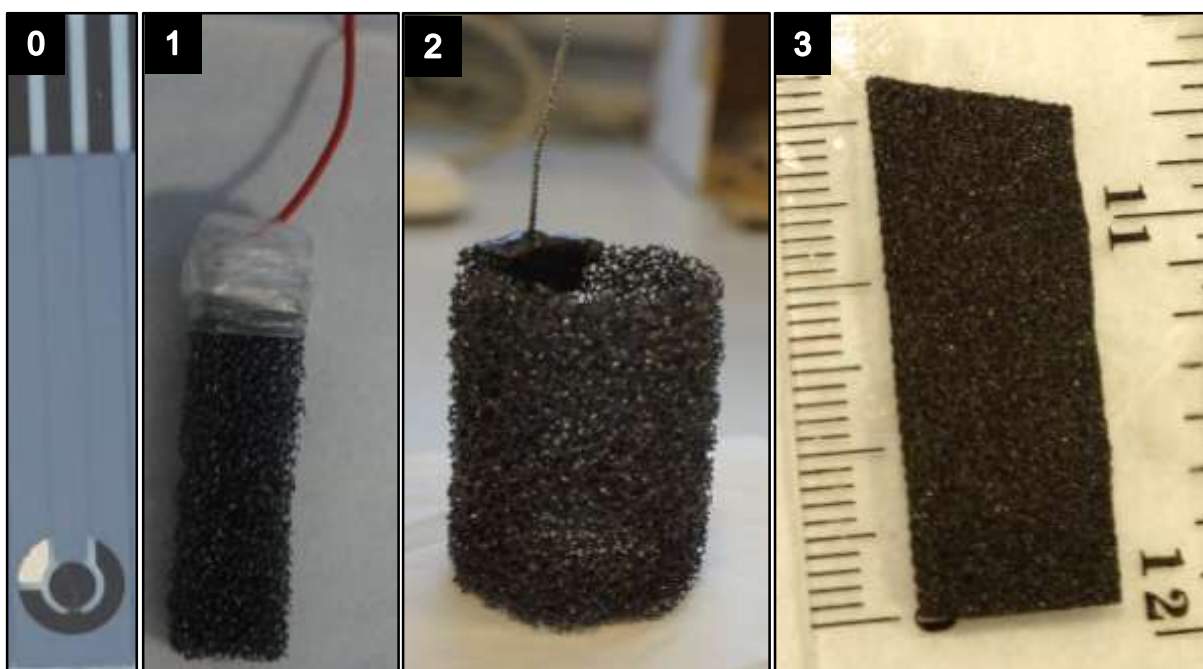
Figure 2.7: Screen printed electrode (SPE) (0), Various types of RVC used in the analysis (1-3).

Figure 2.7 shows the electrode materials used in the study. The physical characteristic (surface area, PPI) of the materials used are stated in the experimental. SPE is used in both probes as a reference to determine if both redox probes are working. For experimental methods, see **(6.1, 6.2 and 6.3)**

As we are not comparing our RVC foam to different systems, k^0 would not be affected by the surface area and this can be seen when we are using Nicholson's equation 3 for working out the diffusion constant. k^0 in these experiments however does depend on the peak to peak difference ΔEP (i.e. the difference in separation of peak of oxidation and reduction). The value of k^0 decreases, as ΔEP gets larger. In general, ΔEP value increases with the increasing scan rate.

The graphs display the raw data that was obtained during the CV of the electrodes. The difference in y-axis value is due to each electrode having a different surface area and this effecting the current value. Therefore, current density plot used to normalise the y-axis of all the electrodes. Current density calculated by dividing the current obtained with the surface area of the electrode.

2.7.1 *Hexaammineruthenium(III) chloride probe*
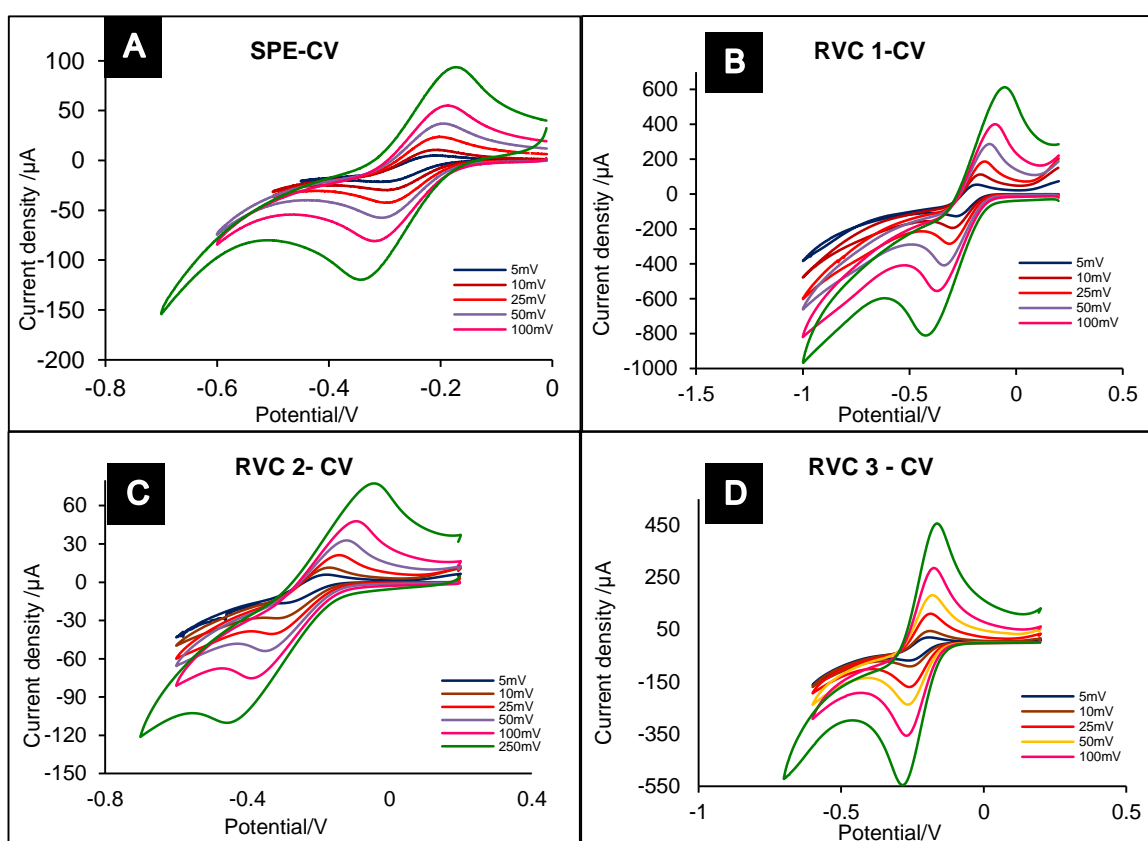
Figure 2.7.1: Cyclic voltammetric graphs of electrodes using hexaammineruthenium(III) chloride probe.

Material Type	k^0 (cm s^{-1})
SPE	1.98×10^{-3}
RVC 1	8.41×10^{-4}
RVC 2	8.41×10^{-4}
RVC 3	2.85×10^{-3}

Table 2.7.1: k^0 of the electrodes in hexaammineruthenium(III) chloride/probe.

The peaks observed at different scan rates of RVC2 are less pronounced when compared to RVC1 and RVC3. This is because RVC2 had the largest surface area hence increased resistance and increased background capacitance. It is interesting to note that RVC3 with smaller surface area is conducting larger current when compared with RVC2, it is possible because RVC 2 (20) has a smaller PPI than RVC3 (70) and hence more surface area. When measuring PPI of RVC, higher number indicates RVC with more pores when compared to a lower number. The effective heterogeneous electron transfer rate constant k^0 calculated for inner

sphere, seems that it is effected by the surface area although indirectly; this is observed when using Nicholson's equation 3 for working out the diffusion constant. ΔEP value is required to calculate k^0 and is affected by the size of surface area.

In general, ΔEP value increases with the increasing scan rate. RVC with larger surface area had a large ΔEP when compared to smaller surface area RVC (or SPE) this is due to more surface for the interactions to take place when using both inner and outer probes.

Table 2.7.1 shows the calculated k^0 although RVC1 and RVC2 have identical k^0, it should be stated that the minimal amount of electrode (RVC2) had to be submerged into the solution before an adequate CV of the electrode could be obtained, anymore submersion of the electrode led to an overload of the current leading to termination of the experiment. Although RVC2 can be used in electrosynthesis, the electrode would have to be positioned very carefully to obtain any useable results. The k^0 of the RVC3 is smaller due to the smaller surface area and value of ΔEP.

2.7.2 Ammonium Iron (II) sulfate hexahydrate
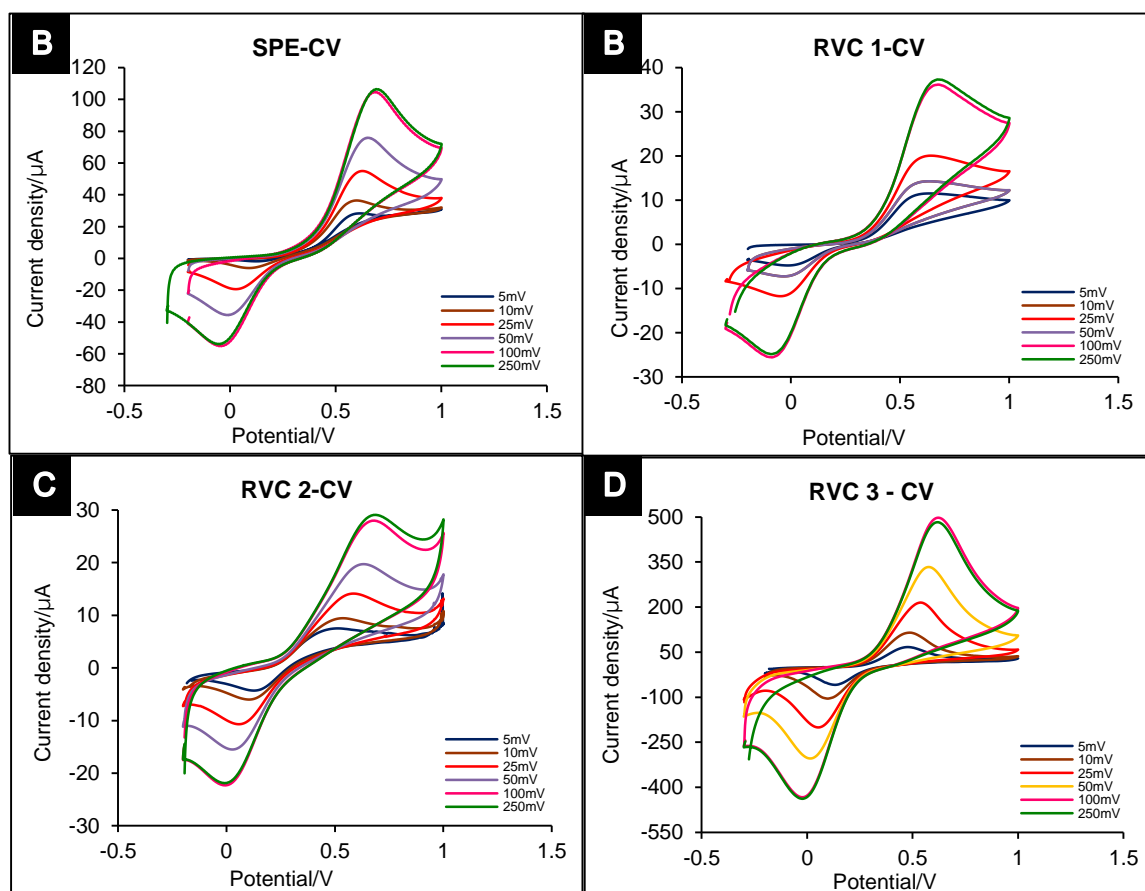
Figure 2.7.2: Cyclic voltammetry of SPE, RVC1, RVC2 and RVC 2 in inner- sphere probe in 1.0 mM ammonium Iron(II) sulfate hexahydrate/0.2 M perchloric acid.

Material Type	k^0 (cm s^{-1})
SPE	2.60×10^{-5}
RVC 1	1.10×10^{-5}
RVC 2	4.98×10^{-4}
RVC 3	4.69×10^{-3}

Table 2.7.2: k^0 from cyclic voltammetry performed in ammonium Iron(II) probe.

Figure 2.7.2 depicts the cyclic voltammetric graphs of SPE and RVC 1-3, it shows reduction occurring first using the inner-sphere probe ammonium iron(II) sulfate hexahydrate probe. In general, the following observation is made that when using inner-sphere probe ΔEP is considerably larger when compared to ΔEP of outer-sphere this is because inner-sphere interactions are more difficult to achieve, whereas interactions take place easily in outer sphere. As mentioned before, although surface area effects the k^0 when using outer sphere probe, similar observations cannot be made when using inner-sphere probe. When we compare k^0 of RVC3 with that of SPE, it indicates that RVC3 is better than SPE due to higher PPI and hence more surface area available for electrochemical interactions. When surface area of RVC2 is compared with SPE and RVC1, k^0 of RVC2 is smaller even though it has considerably larger surface area than the other two electrodes.

2.7.3 SEM Images
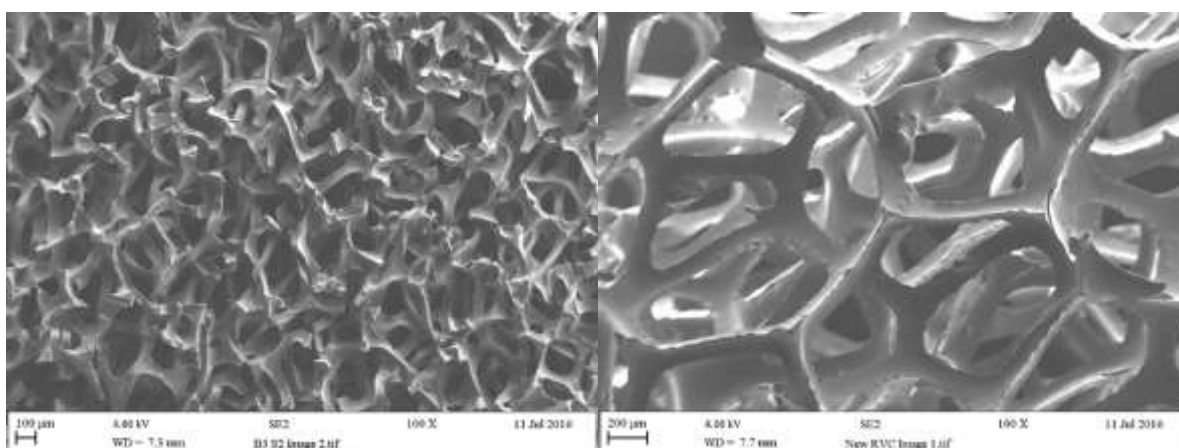
Figure 2.7.3: SEM images of RVC3 and RVC1.

SEM images of RVC1 an RVC3 were obtained, it can be observed in the images that at the same magnification honeycomb structure of RVC3 seems to be more densely packed when compared to the structure of RVC1 hence it had a smaller k^0 in both probes.

2.8 Conclusion

The aim of this chapter was to demonstrate if the selected RVC1 as an electrode was capable of being used in the organic synthesis. Both inner and outer sphere probes were considered for electroanalytical purposes these probes aid to determine if the electrode material being used is viable enough for use. The k^0 of RVC2 and RVC1 in outer-probe is not vastly different and throughout the experiment k^0 of RVC3 was significantly better than the other two RVC. Either RVC3 and RVC2 can be used as electrodes in the future for electrosynthesis. It should be noted that for RVC2 minimum amount of surface area is required for the CV when compared to RVC1, this is due to RVC2 having larger pores and larger surface area when compared to RVC1.

k^0 is the measurement of how fast electrons are reacting with the electrode surface and hence are able to process the electrochemical process from the selected solutions. The k^0 of the RVCs demonstrated that although they were all adequate electrode materials. RVC1 was selected for further experiments due to the reasonable cost and its ability to measure the electron interactions, the k^0 was within the accepted range (10^{-3} and 10^{-4}). RVC2 was not selected for further experiments as minimal amount of electrode had to be used to gather any electrochemical information in previous experiments and this would pose further complication when used in the organic synthesis. RVC3 was not selected due to the availability of the electrode materials in the laboratory and the cost.

2.9 Future Work

It was observed in the experiments that RVC3 gave the best k^0 when compared to the other two RVCs, it would be interesting to investigated the behaviour of various PPI of RVC to be used in organic electrosynthesis. As generally it is found in literature that although an electrode might have a larger or a smaller surface area, it is not necessarily the case that interaction will be occurring with the available surface area. Further research can also take in account not only carbon based RVC electrode but also metal based electrodes. Scanning electronic microscopy (SEM), Transmission electron microscopy (TEM) can be used to determine the internal composition of the RVCs.

Chapter 3 – Pencil Drawn Electrodes (PDEs)

3.1 Introduction

The viability of Pencil Drawn Electrodes (PDEs) compared with RVC electrodes for electrosynthesis will be studied in this part of the research project. They were selected because, these electrodes previously have not been used in organic electrosynthesis, they are only used in analytical chemistry for electrochemical sensing. One of the points that set PDEs apart from other electrode is that they can be fabricated to any geometric size and shape using ordinary writing pencils.

Carbon-based electrochemistry has received notable interest over the last two decades.[70] There are exciting possibilities of using carbon-based devices as they can exhibit similar or enhanced performance when compared to their traditional counterpart of using noble metal based sensors.[70,84] Within the fields of carbon nanotubes, highly ordered pyrolytic graphite,[85-86] mono- and few- layer graphene[87-89] there is a wealth of knowledge being obtained using carbon-based electrochemical devices.[90-91] An accurate composition can contribute to selective, sensitive, experimentally straightforward and inexpensive electrochemical derived sensors. As PDEs have the ability to convert chemical information into an electrical signal (such as showing the oxidation and reduction peaks), this property of PDEs has made them an interesting electrode to be investigated.[10] The utilisation of pencil drawing technology can be incorporated into these electroactive materials.[70] There is a constant focus towards the production of an improved analytical sensing platform and minimising the cost associated with the creation of sensing platforms throughout the literature and industry by utilising commercially available pencils.[70] A scientific revolution has occurred due to the development of portable miniaturised analytical devices.[92] One of the industries that has benefited from the screen-printed sensors is the glucose sensing market (for diabetes) that has combined the screen-printed electrodes with handheld sensors.[93-94] A low cost of PDEs and of screen-printed electrodes would allow more organic chemist to adapt this technology by investigated the cyclic voltammetry of various compounds (varying functional group and complexities) and allowing them to further use electrochemistry as a part of synthesis.

3.2 Pencil Drawn Electrodes (PDEs)

Pencil Drawn electrodes (PDEs) were created as an alternative to using pencils as standalone "lead" electrodes. Many electrochemical applications reported in the previous literature were focused on detection of ascorbic acid, dopamine and morphine, where a pencil electrode was employed.[70] However, there are drawbacks in employing standalone pencils as working electrodes due to their lack of tailorability within the design, the bulky/large nature and control of working area.[90] Electrochemists are continually striving for novel electrode configurations and PDEs appeared recently as a very interesting alternative.[95] These electrodes are an economical approach as one can potentially draw their own electrode and electrochemical systems of any dimensions or specification.[70] There is a high percentage of graphite in commercial drawing and writing pencils, and the pencil "lead" can be used as an electrode itself, making the electrode material very cheap compared to Nobel metals.[95-96] Using the commercially available pencils and a variety of substrates (such as paper or plastic) sensing platforms can be fabricated in minutes.[70] Pencil are classified and "graded" on a scale from H to 9B as shown in Figure 1. The composition of pencil "lead" is an amalgamation of graphite, clay and wax. The composition between harder and softer pencil leads arises from the difference in blackness from the various relative fractions of the graphite present in the composition of the "leads".[89] Hence the ability of the pencil to provide the sensing platforms is heavily reliant on the amount of graphitic material transferred to the substrate.[89]
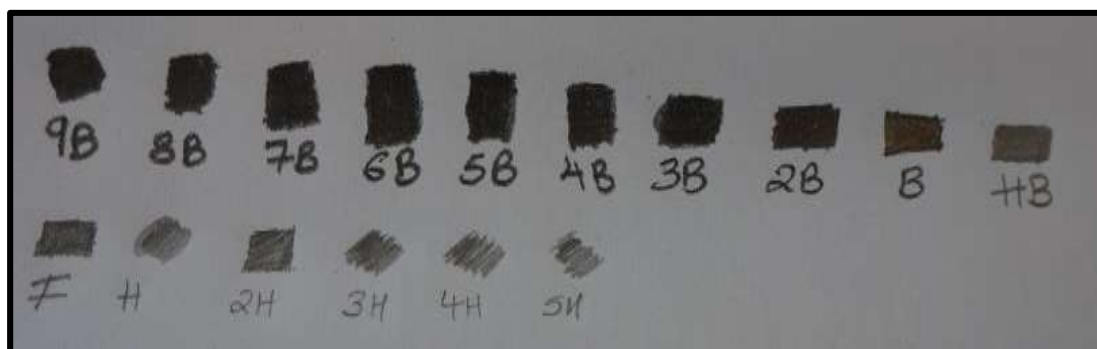
Figure 3.2.1: Graphite deposition using a variety of commercial grade pencils.

Table 3.1 provides a summary of the current research into the electroanalytical applications of PDEs but also shows that the interest in utilising PDEs has amplified.[70] Most of the research that is emerging has been focused on either utilising PDEs towards a specific sensing application or characterising the electrochemical properties of the PDEs.[92,97-98] Dossi et al.[99] have studied the detection of ascorbic acid using PDEs upon paper substrates. The group also investigated the electrochemical detection of analytes such as potassium ferrocyanide,[100] paracetamol[100], 1,2-hydroxybenzene,[99] dopamine[94], and orthodiphenols in edible oils samples.[70] Honeychurch[92] demonstrated that Lead (II) could be detected in canal water samples using PDEs on a polyvinyl chloride substrate.

Electrode Fabricated	Pencil and Substrate utilised	Number of draws	Target analytes	Analytical method	Ref
Pencil-drawn working macroelectrode	Commercially available Staedtler Mars tradition pencils fabricated upon an ultra-flexible polyester substrate (6B, 5B, 4B, 3B, 2B, B, HB, H, 2H explored)	1–10 draws	Ammonium Iron(II) sulfate, p-benzoquinone, Hexaammine-ruthenium(III) chloride, Potassium ferricyanide, and simultaneous detection of lead(II) and cadmium(II) ions	Anodic stripping voltammetry and Cyclic voltammetry	70
Pencil-drawn working and reference macroelectrodes	Commercially available Derwent pencils upon an ultra-flexible polyester substrate (HB, B, 2B, 3B, 4B 7B, 8B, 9B explored). Reference electrodes have been drawn with a HB and compared to screen printed alternatives.	60 draws	Hexaammine-ruthenium(III) chloride, potassium ferrocyanide, ammonium iron(II) sulfate, dopamine and paracetamol.	Cyclic voltammetry	89
Pencil-drawn working macroelectrode	Derwent (grade '6B' only) upon polyvinyl chloride substrate	Not stated	Lead(II)	Anodic stripping Voltammetry	92
Pencil-drawn working Macroelectrode with pseudo reference and counter electrode	Working electrode was a bespoke "pencil" manufactured utilising a mixture of graphite, sodium bentonite and potassium silicate, then doped with decamethylferrocene or cobalt(II) phthalocyanine and drawn upon paper substrates. Additional counter and reference electrodes are also drawn onto the substrate.	4 draws	Cysteine and hydrogen peroxide	Cyclic voltammetry and Linear sweep voltammetry	97

Pencil-drawn macroelectrode	Derwent, Staedtler Mars Lumograph, FILA and Koh-i-Noor Hardtmuth (HB, B, 2B, 3B, 4B, 6B, 8B explored) upon paper substrates.	Not Stated	Ascorbic acid, sunset yellow and Potassium ferrocyanide.	Thin-layer chromatography with amperometric detection and cyclic voltammetry	98
Pencil-drawn dual electrode with pseudo reference electrode	Staedtler Mars (grade '3B' only fabricated upon paper substrates.	Not Stated	Ascorbic acid, dopamine and paracetamol	Thin-layer chromatography with amperometric detection and cyclic voltammetry	100
Pencil-drawn working macroelectrode	Range of commercially available pencils explored Derwent, Koh-I-Noor Hardmuth, Linex ® and Castle Art Supplies. The pencil grades used were 9B, 8B, 7B, 6B, 5B, 4B, 3B, 2B, B, HB, F, H, 2H. The electrode compared with RVC electrode.	5 to 100 draws	Hexaammine-ruthenium(III) chloride, Ammonium iron(II) sulfate and organic compounds.	Cyclic voltammetry and galvanostatic method.	This work

The capacity to draw one's electrode onto a range of surfaces is attractive as not only the PDEs potentially allows for simple, efficient, inexpensive and portable sensors to be developed but it would also enable versatility and regulation of the working area.[70]

Recently the Banks' research group characterised and examined for the first time how the electroanalytical capabilities of the PDEs can be affected by the number of layers and the grade of pencil.[70] A range of commercially available Derwent and Staedtler (pencil brands) pencils were used to fabricate the PDEs and analysed.[89] They demonstrated that heavy metals such as Lead(II) and Cadmium(II) can be detected using the PDEs.[70] Further research compared how the electrochemical sensing capabilities and the electron transfer properties were varied between different batches of the same pencils demonstrating a lack of reproducibility in the composition of pencils used for fabricating PDEs. They compared the feasibility of PDEs to graphitic based screen-printed electrodes for the detection of dopamine and paracetamol. Furthermore, screen-printed alternatives were also compared with the pencil drawn working electrodes examining the overall feasibility and suitability of the PDEs drawn as a full electrode system, concluding that PDEs were comparable with SPE alternatives when pencils are functional. [70]

Inspired by the interest in utilising PDEs as an electroanalytical device we explore how PDEs can be used in the organic electrosynthesis. To the best of our

knowledge, all the research conducted using PDEs have involved aqueous chemistry. Herein we report the viability of using PDEs in both an aqueous and organic environment and whether the PDEs can be used in electrosynthesis.

3.3 Aims

The aim of the study is to find the optimum pencil grade (and number of graphitic layers applied to the substrate) to develop a PDE for used in organic electrosynthesis. Data obtained with the PDEs will be compared with the electroanalytical of RVC such as the ability of the electrodes to measure oxidation and reduction in a reversible CV. Furthermore, we explore if there is any difference in the electrochemical responses between the brands of commercial pencils.

3.5 Results and Discussion

The reasoning behind why a certain pencil is chosen is largely neglected in the current literature.[70] The next sections will include comparisons of pencil grades and number of draws within each brand (full details are given in the experimental section, 6.1, 6.2 and 6.5).

The first step of the experiment was to determine the optmised PDEs and pencil grade (2H, H, F, HB, B, 2B, 4B, 5B, 6B, 7B, 8B and 9B) from each brand. Outer sphere redox probe (see chapter 2.5.1) hexaammineruthenium(III) chloride was used to electrochemically characterise individual pencil grades *via* cyclic voltammetry at scan rate 25 mV/s^{-1}, as it is the middle scan in a normal scan rate study.[89] The analysis was performed with the electrodes being "pencilled in" 5, 10, 20, 60 or 100 times. This was to analyse which grade and draw gives rise to the optimum electrochemical properties.

Once the optimised PDEs and pencil grade from each brand was selected, the second step was to perform a full scan rate study (scan rates used 5 mV/s^{-1}, 10 mV/s$^{-1,}$ 25 mV/s$^{-1,}$ 50 mV/s$^{-1,}$ 100 mV/s$^{-1,}$ 250 mV/s^{-1}) first using the outer sphere redox probe and then inner-sphere redox probe. Comparing the pencil grades from different brands.

3.5.1 Castle Art Supplies
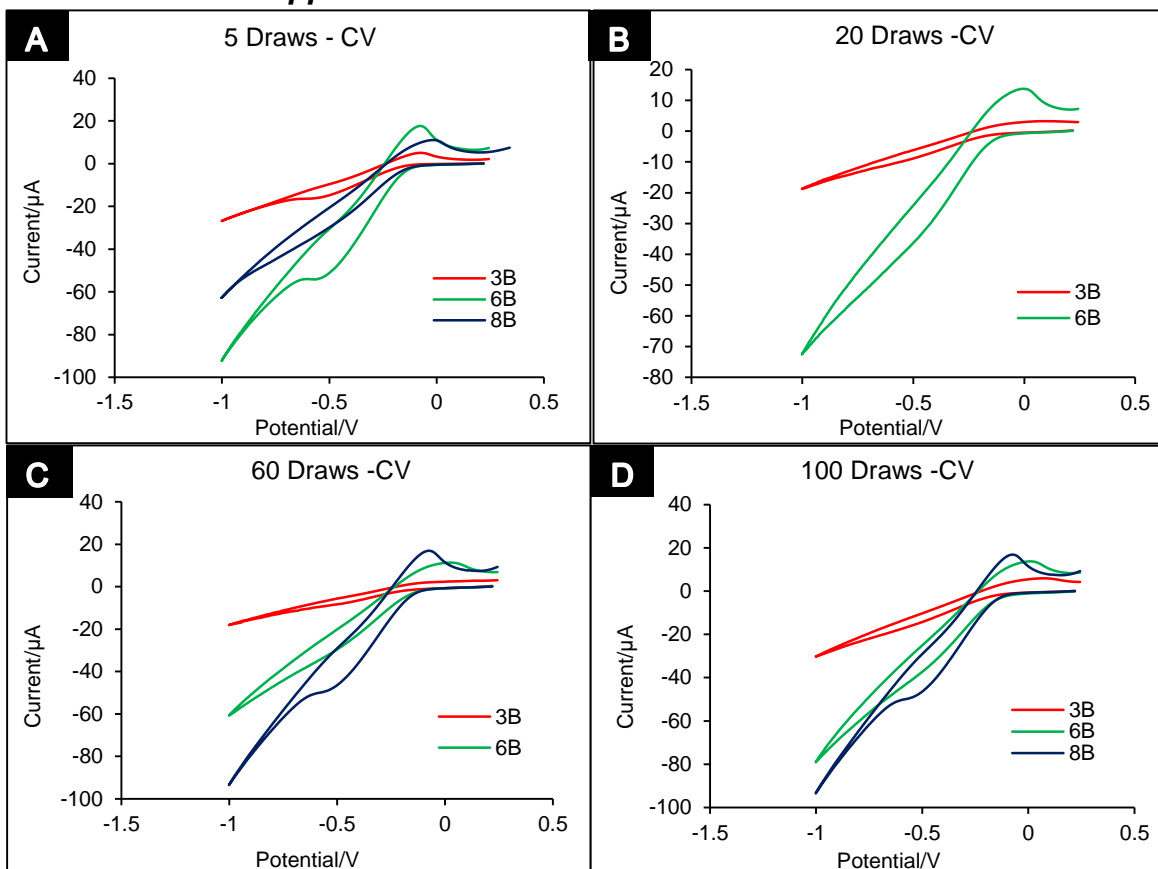
Figure 3.5.1: Cyclic voltammetry of various draws and pencil grade in 1.0 mM of hexaammineruthenium(III) chloride/0.1 M KCl. Castle art supplies pencils. Scan rate: 25 mV s^{-1}.

Figures 3.5.1A-3.5.1D shows cyclic voltammogram(CV) recorded at 25 mV s^{-1} using redox probe hexaammineruthenium(III) chloride/ 0.1 M KCl. Figure 3.5.1A-D shows PDEs fabricated applying 5 Draws, 20 Draws, 60 Draws and 100 draws receptively.

When comparing the pencil grades in Figure, 3.5.1A PDE drawn using 6B pencil gives the best response due to decreased peak to peak separation and increased reversibility when compared to the other two pencil grades (3B and 8B). When comparing in general 6B to 8B (Figure 3.5.1A-3.5.1D), 6B provides better voltammogram than 8B even though it is a lower pencil grade. It is likely that more graphite was deposited onto the substrate when using 6B pencil than 8B for the fabrication of PDEs. It might be because in the composition of 8B pencils there is more clay that was deposited onto the surface after drawing which leads to not creating an adequate conductive layer upon the paper substrate.

Cyclic voltammogram recorded for PDE fabricated using 8B pencils after applying 20 draws is not included within Figure 3.5.1B because it showed considerably larger current when comparing to the other pencil grades and would have skewed the graph significantly whereupon the CV of 3B and 6B would have been difficult to distinguish. 6B does not show a reversible scan in this Figure this could be more deposition of clay rather than graphite.

Figure 3.5.1C and 3.5.1D shows that 8B provides a better response at higher draws when compared to lower draws. We can also observe a smaller peak to peak separation, and it gives improved reversibility. More graphite is found in the composition of pencil's lead at a higher pencil grade (i.e. 9B > 2H). This can be observed by comparing 8B to 6B, at more draws the electrochemical response of 8B increase indicating more graphite being deposited onto the PDEs.

It is worth noting that 6B gave the best response and reversibility only at 5 draws, however in the subsequent layers only oxidation of redox probe was observed, and no reversibility can be seen, this is because the PDEs cannot be reproduced. Thus in summary 8B from this batch was selected for further analysis as the CV for this grade gave the best peak to peak separation at higher draws but also showed improved reversibility when compared to the rest of the pencil grades that were analysed within this batch of pencils
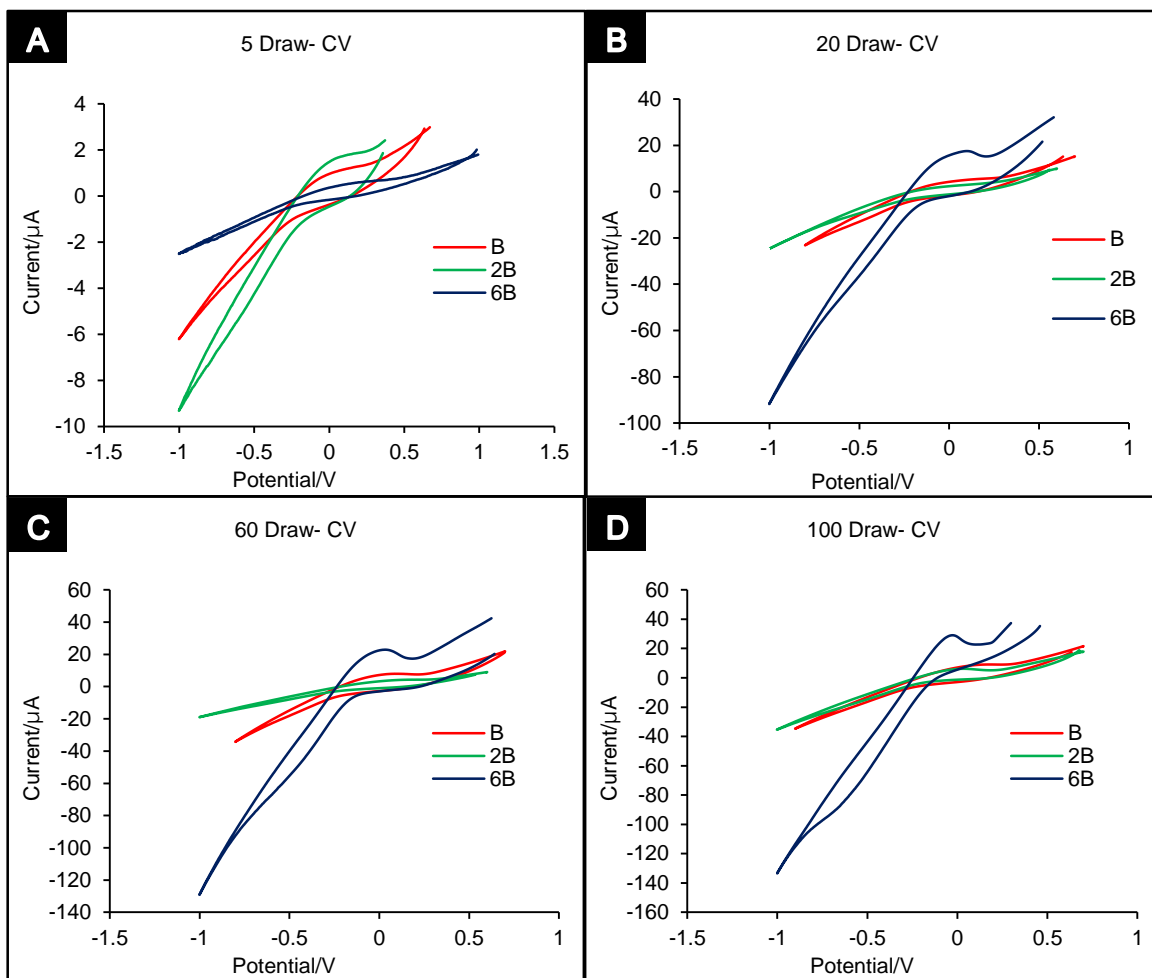
3.5.2 Koh-I-Noor
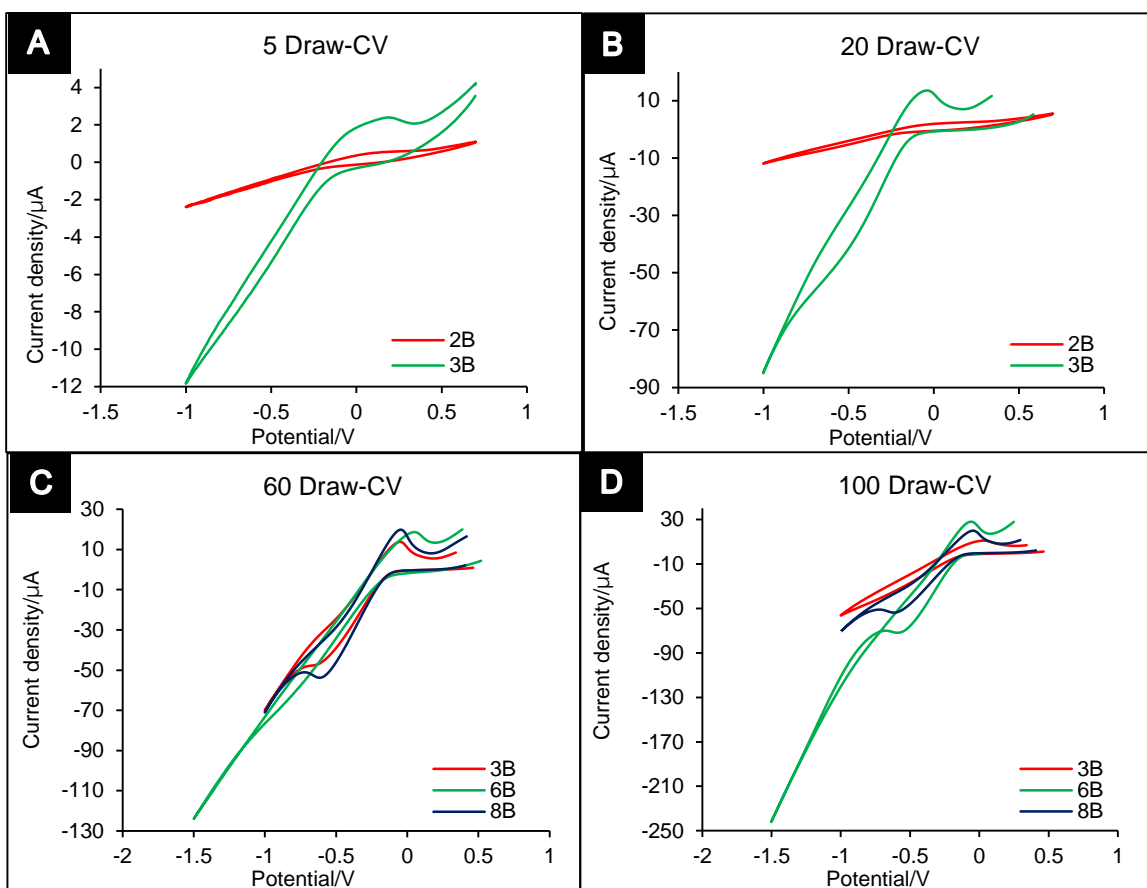
Figure 3.5.2: Cyclic voltammetry of various draws and pencil grade in in 1mM of hexaammineruthenium(III) chloride/0.1M KCl. Koh-I-Noor pencils.

Figure 3.5.2A and 3.5.2B only show the pencil grade 2B and 3B because higher pencil grade PDEs did not provide effective electrochemical responses, possibly due to little graphite transfer onto the PDEs at such lower draws. Pencil grade 2B and 3B show an electrochemical response in detecting just the oxidation, but there is no detection of reduction and hence no reversibility is observed in these pencil grades. It can be observed in Figure 3.5.2C & 3.5.2D that the pencil grade show reversibility of 6B and 8B but the reversibility of 3B and 2B declines.

Hence pencil grade 6B and 8B at 100 draws was selected for performing scan rate study. The reasoning behind using 100 draws is that although both draws show reversibility the peak to peak separation is smaller and hence better defined at 100 draws when compared to 60 draws.

34

3.5.3 Linex

Figure 3.5.3: Cyclic voltammetry of various draws and pencil grade in 1.0 mM of hexaammineruthenium(III) chloride/0.1 M KCl. Linex pencils.

As we can observe from the Figures 3.5.3A to 3.5.3D the pencil grade does not seem to have a significant effect on improving the reversibility of this brand's PDEs. Although 6B improves slightly at higher draws, however, it is not significant enough, and the peak to peak separation is large when comparing with the other 6B pencil brands. It might be that the quality of graphite is not adequate and hence the poor conductivity of the redox probe. The PDEs are also very resistive, the peak to peak separation was poor and little to no reversibility was observed in these PDEs hence no pencil grade was selected from this brand.

3.5.4 Derwent

The CVs obtained of PDEs from the Derwent brand did not provide effective electrochemical responses, because the graphite and clay composition within the pencil lead are not creating an adequate conductive layer upon the surface. It might also be that there is not enough coverage of graphite onto the PDEs. Although they were conductive, there was no reversibility even when a higher grade of pencil and more draws was used. The current of each draw within a pencil grade also varied which distorted the CVs graphs and hence the graphs are not included.

3.5.5 Scan Rate study with hexaammineruthenium(III) chloride
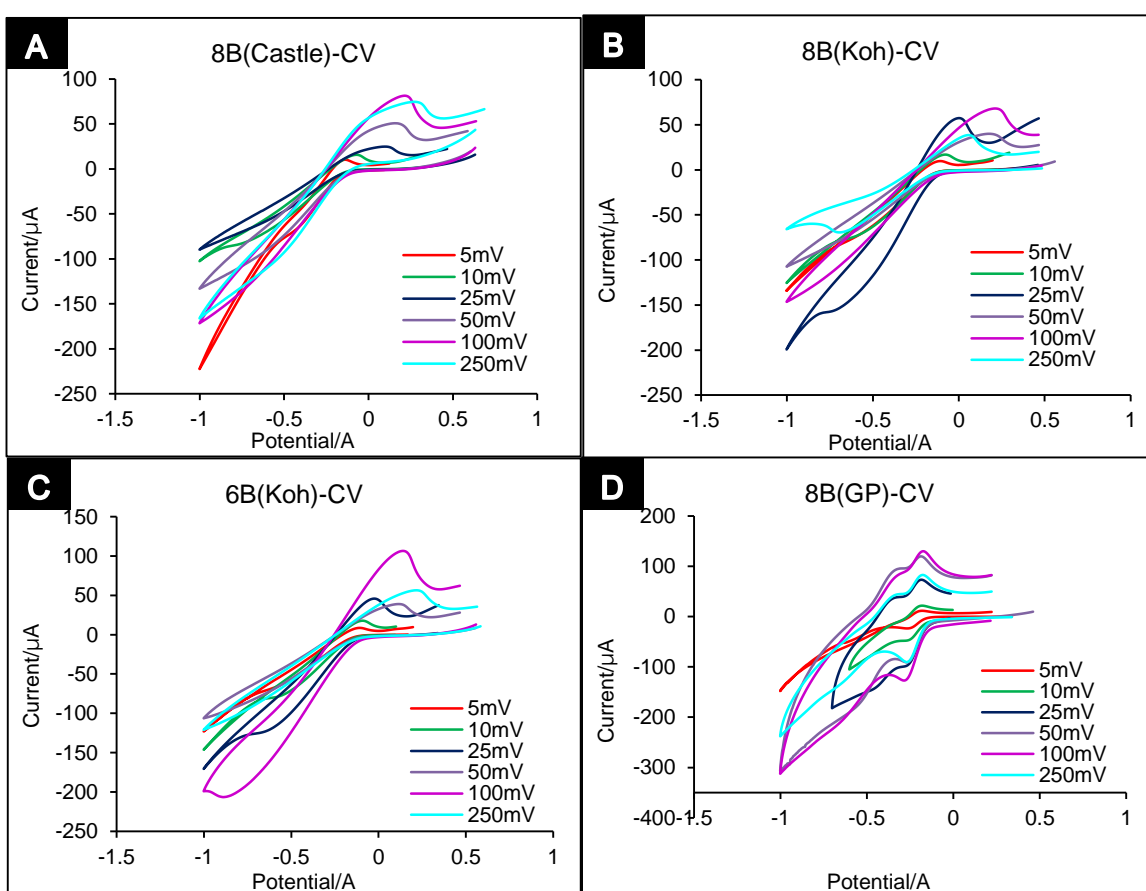
Figure 3.5.4: Scan rate study of 100 draws various pencils in 1.0 mM of hexaammineruthenium(III) chloride/0.1 M KCl. Image D is the scan rate study of the actual pencil itself utilised as electrode.

Figure 3.5.5: Pencil as electrode.

Scan rate study of PDEs using the selected pencils was carried out in 1mM of hexaammineruthenium(III) chloride to determine if the pencils would give a similar response at different scan rates (see experimental for the selected scan rates) and not just at 25mV s^{-1}.

Figure 3.5.4A shows scan rate study of PDEs fabricated from 6B pencil grade. Castle brand shows high resistivity, although oxidation is observed no reversibility is seen in most scan rates. The only scan rate that shows reversibility is at 10mV s^{-1} and a peak to peak separation is visible as well. CVs of PDEs fabricated from 8B Koh-I-Noor are shown in Figure 3.5.4 6B scan rate at 25mV s-1 and 250mV s^{-1} show not only reversibility but also small peak to peak separation. When comparing the Scan rate only, 250mv s^{-1} shows low resistivity. Scan rate 100mV s^{-1} and 25mV s^{-1} of 3.5.4B PDE from Kho-I-Noor in Figure 3.5.4C show reversibility. However, Scan rate 100MV s^{-1} has a greater peak-to-peak separation and is more resistive than the rest of the scan rate.

Figure 3.5.4D shows scan rate study where the pencil itself was used (Figure 3.5.5) as an electrode. Reversibility is seen at all scan rates and peak-to-peak separation is also visible even though it is considerably large. Two peaks are observed at oxidation; this could be due to an impurity of the solution or from the pencil itself.

Although the CVs are considerably wider (larger capacitance) when compared to the scan rate study. It should be noted that the pencils are not designed for purposes electrochemical analysis.

Therefore, looking at all the scan rate studies and comparing the CVs. It was decided that PDEs fabricated from pencil 8B would be used in the organic application part of the project; because the highest scan rate showed low resistivity, reversibility and the smaller peak to peak separation. Pencil as an electrode will also be used for the electroorganic synthesis.

3.5.6 Scan rate study with Ammonium Iron(II) sulfate hexahydrate
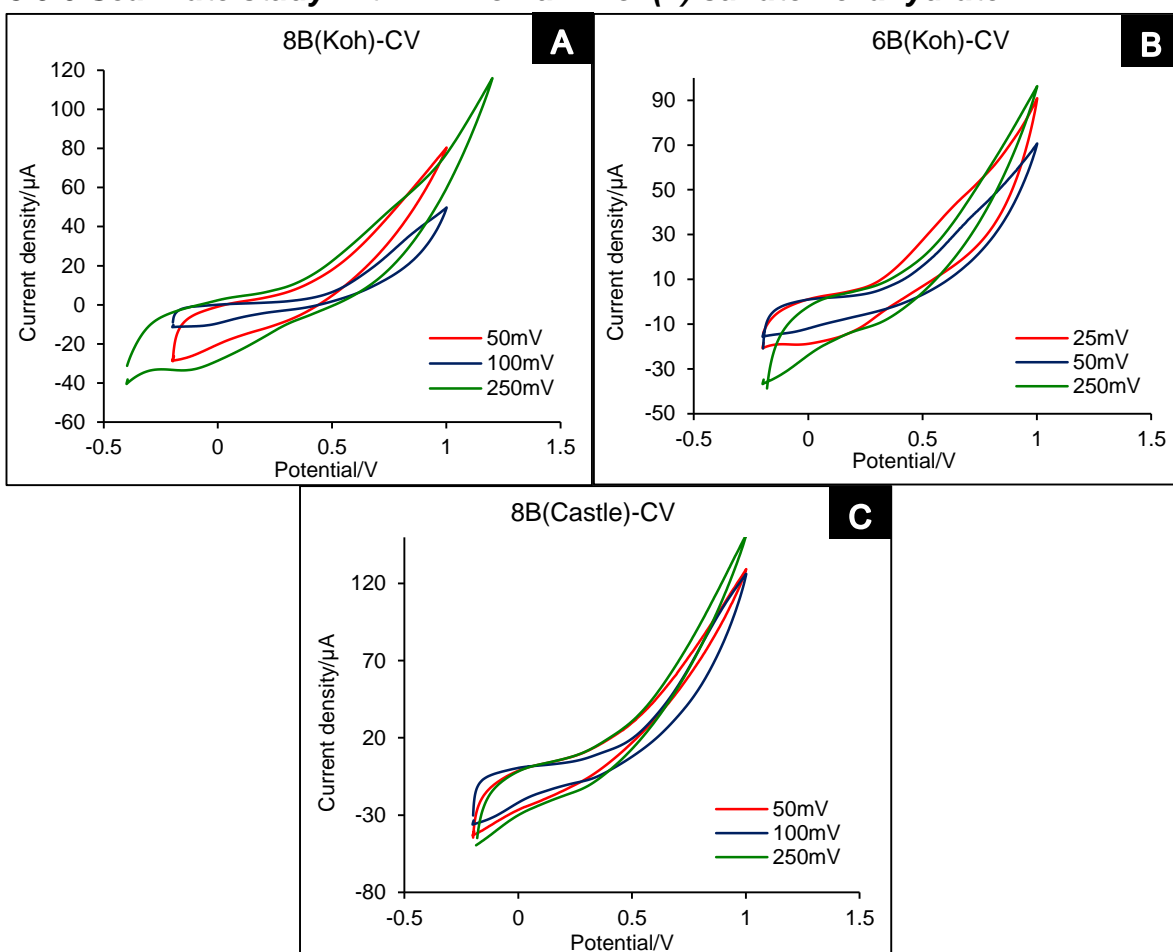
Figure 3.5.6: Scan rate study of 100 draws in 1.0 mM ammonium Iron(II) sulfate hexahydrate/0.2 M Perchloric acid.

Scan rates conducted with the inner-sphere (section 2.5.2) probe in 1.0 mM of ammonium Iron(II) sulfate hexahydrate showed a poor response. A similar type of response was seen in literature by Foster *et al.*[63] The CVs show that although the PDEs are conductive, no reaction is occurring upon the surface as far as we can observe. This could be due to the surface composition of the PDEs and not enough coverage.

3.6 Conclusions

In this chapter, the fabrication and characterisation of the PDEs with outer-sphere probe has been investigated. The effects of the number of draws, pencil grade and brand were also considered. Pencil as standalone electrode has been utilised. Scan rate study performed with both the inner and outer sphere probes on the final selected PDEs.

PDEs provided beneficial information regarding the electrochemical signatures when utilising the outer-sphere probe (which are sensitive only to the electronic structure of the electrode surface). However, when using the inner-sphere probe, limited electrochemical signatures is given (which are sensitive largely to surface groups/oxides and to the surface composition) this could be due to the composition/surface of the PDEs as demonstrated by the scan rate study.

PDEs are "green", cheap to make and simple. However, there are downsides to the fabrication of PDEs as it is not only time consuming, but they are also not reproducible. An example of this would be the observation made during the experiments of pencil grade 8B from the castle art supplies. The initial scan was carried out on 100 draws at 25mV s^{-1}, it gave reversibility and small peak to peak separation, however when the same was repeated for the scan rate study, no peak to peak separation was observed only the oxidation was seen. However, as stated before the pencils utilised in the fabrication of the PDEs are not designed for electroanalytical purposes, and there is uncertainty to the purity of the graphite contained in the pencils how much of composition of the pencil is graphite, clay and wax. Further research is ongoing on PDEs to gain more insight into their characterisation and applications in variety of fields.

Chapter 4 will look at the viability of using the PDEs and the pencil as an electrode to perform organic electrosynthesis and performing cyclic voltammetry on organic

compounds. PDEs will be compared to with RVC to determine if they are viable electrodes to be employed in electrosynthesis.

3.7 Future Work

Transmission electron microscopy (TEM) can be utilised for the imaging purpose of the PDEs once the CVs have been performed on the electrodes. A further technique that can also be used is Raman to observe any changes to the electrode that has been made during the electrochemistry and to observe the deposition of the compounds on it. Scanning electronic microscopy(SEM) of the draws could be carried out to inspect how much graphite is deposited onto the surface. Further exploration could be perhaps testing the variety of substrate for comparing to see which supporting would work best.

## Chapter 4 – Cyclic Voltammetry and Potentiostatic method results and discussion

4.1 Amides

The most developed electrosynthetic method is amide oxidation.[16,46,101] Anodic oxidation of amides, carbamates, lactams and *N*-acylated amino acids has proven to be complementary technique for the synthesis of biologically active compounds (see section 1.5).[21] However, questions such as the selection of electrochemical parameters, e.g. how does the reaction conditions effect the end product formed, still exist about the overall synthetic utility of these reactions.[20]

The tertiary amides used in this study were selected as they meet the criteria of Shono oxidation (the amides can be oxidised to an *N*-acyliminium ion and can be captured by various nucleophiles). All the selected amides vary steric effects, and electro donating/withdrawing ability of an attached group on the amide-containing compound can affect the oxidation potential of the compound.

Several of the selected amides have two available C-H activation sites. Compound **7-9** have two aromatic ring systems; it will be interesting to see where C-H activation would occur. Electrosynthesised amides have been reported by conventional synthesis to afford a methoxylated product for comparison of ^{1}H-NMR to aid the complex product mixture identification.

Complicating matters further, there features associated with the amide group such as its planarity. There is an area of delocalization (Scheme 4.1.1) into the carbonyl due to the nitrogen lone pair electrons. The lone pair on the amide's nitrogen is in a fixed position in the system making it less available for protonation or reaction with any electrophile. The delocalisation strengthens the C-N bond and takes on a partial double bond character. Thus rotation about the C-N bond is no longer free. These properties together and the delocalisation make the amide group more stable and less reactive.[102]
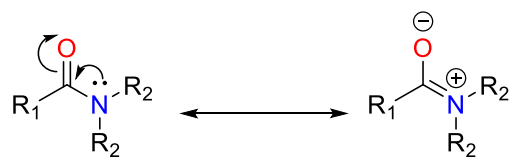
Scheme 4.1.1: Delocalisation of the nitrogen lone pair onto amide bond.[102]

Observations made with X-ray structures shows that the amide group is planar. Other techniques such as electron diffraction also show that simple (non-crystalline) amides have planar structures. Using *N,N*-dimethylformamide (DMF) we can demonstrate why splitting of signals occurs in NMR spectrum of amides.

When comparing the single bond length (149 pm), we observe that C–N bond length to the carbonyl group is closer to that of a standard C–N double bond (127 pm) rather than single bond length. The restricted rotation about the C-N bond is due to this partial double bond character.
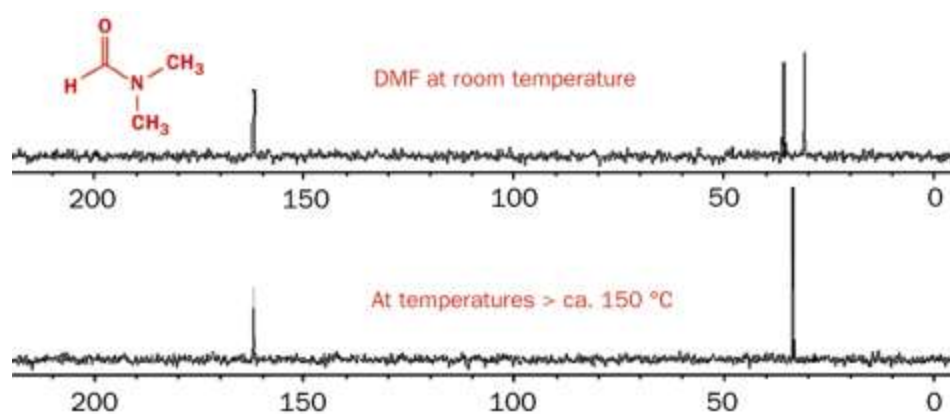
Figure 4.1.2: Carbon NMR spectrum of DMF at room temperature and at 150 °C.[102]

C-N bond is locked at room temperature as if were a double bond, the amount of energy required to rotate (88 kJ mol^{-1}) the C-N bond in DMF (or other amides) is not available at room temperature and hence the splitting of signals. This can be demonstrated when looking at the carbon NMR spectrum (figure 4.1.2) of DMF. Three signals are visible (the two methyl groups on nitrogen are different) rather than two. if free rotation was possible about the C–N bond, only two signals would be observed in the NMR spectrum.

However, if the ^{13}C-NMR spectrum was to be recorded at higher temperatures, only two signals will be seen as at higher temperature sufficient energy is available to overcome the rotational barrier and allowing the two methyl groups to interchange. This will complicate the interpretation of the reaction products and therefore the examples selected are known to have at least one methoxylated analogue ^{1}H -NMR spectra known from alternative syntheses. The production of an alpha-methoxylated product will distort the rotamer abundances around the amide from 1:1

4.2 Purchased and synthesised amides
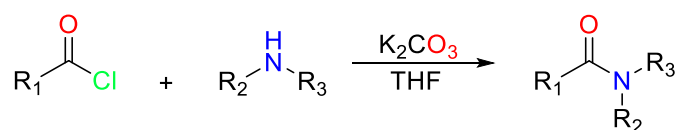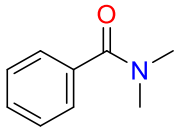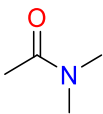
Entry	Amides	Products	Yields (%)
1	1		91%
2	4		88%
3	5		81%
4	7		59%
5	8		47%
6	9		78%

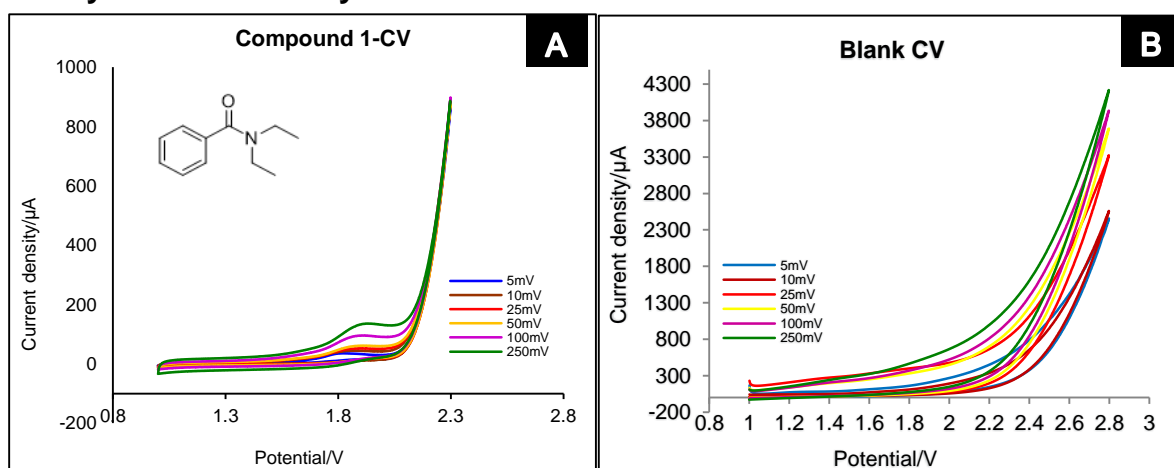**Table 4.2.1** Synthesised amides and the yield obtained.

Synthesise of amides is a reaction between acyl chloride and secondary amine, followed by extraction and column chromatography to isolated the pure compound. Compounds **1-5** gave excellent yields. Compound **8** has a low yield, when compared to compound **9**, even though the reaction conditions were the same, this is because the chlorine on the aromatic ring makes the carbonyl electron deficient, increasing

$\delta+$. Whereas the methyl group on the compound's carbonyl increases the electron density and therefore % yield reduces significantly. The yield obtained with compound **7** is averaged between compound **8** and **9** this is because there are no additional groups attached to it.

Entry	Amide	Amides
7	2	(1-methylpyrrolidin-2-one structure)
8	3	(N,N-dimethylbenzamide structure)
9	6	(N,N-dimethylacetamide structure)

Table 4.2.2 Amides purchased for the electrosynthesis.

4.3 Cyclic voltammetry

Figure 4.3.1: Cyclic voltammetry profile of compound 1 (20 mmol/l) in (9:1) MeCN: MeOH with 0.5 M/TBAP as electrolyte. CV profile of blank, mixture of MeCN and MeOH (9:1) ratio with 0.5 M/TBAP as electrolyte.
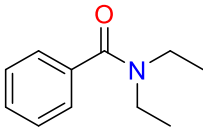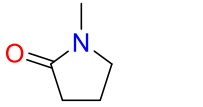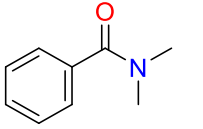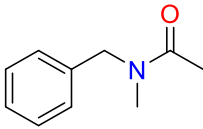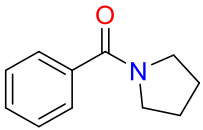
To understand the oxidation potentials of compounds, a scan rate study (over range of scans) using cyclic voltammetry is conducted. A blank (solution containing the solvents and electrolyte) is carried out to eliminate the solvent potential from the CV of the compounds. No peaks of solvent are visible in figure 4.3.1a, the oxidation peaks present are of the compound. To determine if process is diffusional (since $I_p \sim \upsilon^{1/2}$) or absorbed in nature ($I_p \sim \upsilon$) a plot of peak current (I_p) is plotted against
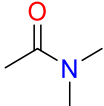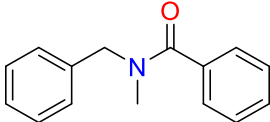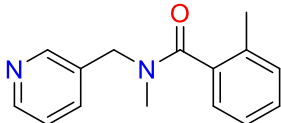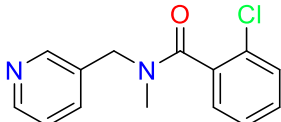
scan rate (υ) . Additional plot of peak current against the √υ is also plotted. The most linear graph indicates the dominant process.[67]

Analysis of the data presented in figure 4.3.1a shows linear response (Ip/A = 4.18×10^4 A/vs^{-1})$^{1/2}$ + 4.20×10^{-6}A; N = 5; R^2 = 0.997) in this case indicates a diffusional process. The diffusional process indicates that it is fully irreversible electron transfer process (not stirred) and hence Randles-Ševćik equation is used to calculate Ip/A.

$$I_p = \pm 0.496(\alpha n')nFAC\left(\frac{FDv}{RT}\right)^{1/2}$$

Geometric area of electrode (cm^2) A, transfer coefficient (usually assumed to be close to 0.5) α, total number of electrons transferred per molecule in the electrochemical process n, the number of electrons transferred per moles before the rate determining step n', F is the Faraday constant, R is the universal gas constant and T is the temperature the electrochemical process is performed at. The voltammetric signal (I_p) will be significantly affected by numerous factor (such as temperature, voltammetric scan rate, the diffusion coefficient and the concentration of the analyte under investigation and the electrode area). Table 4.3.1 shows oxidation potential obtained at 5mV/s of compounds differs in different electrolytes.

Entry	Amides	Oxidation Potential at 5mV/s using TBAP	Oxidation Potential at 5mV/s using LiClO$_4$
1		1.9 V	1.8 V
2		1.7 V	No peaks observed
3		1.7 V	No peaks observed
4		1.7 V	1.7 V
5		1.8 V	1.8V

6		1.8 V	1.8 V
7		1.7 V	1.8 V
8		1.8 V	1.9 V
9		1.8 V	1.9 V

Table 4.3.1: Oxidation potentials of compounds in (10:1) MeCN: MeOH with 0.5 M/TBAP as electrolyte and 20mmol/L of compound. 0.5 M/LiClO$_4$ as electrolyte in (10:1) MeCN: MeOH and 20mmol/L of compound.

The high oxidation potential of **6** is due to carbonyl group which is not stabilised by an aryl system, when compared with **3**. The oxidation potential of **1**, **7** - **9** is between 1.7 V and 1.9 V this is because, the potential C-H activation sites are surrounded by aromatic systems, hence making the reaction site more sterically hindered and more difficult to allow C-H activation.

Compounds with the lowest oxidation potential are **2** - **4**, making them more easy to oxidise as the electronic properties of the aromatic rings do not have much effect on the C-H activation site, and the sites are less sterically hindered (compared to **7-9**) but also stabilised by the aromatic rings.

4.4 PDEs and pencil

To measure CV of **1**, PDE was used as electrode (Procedure 6.12), however due to the graphite or polymer backing absorbing the organic solvent, the experiment was terminated and no data was obtained. The pencil as a standalone electrode was also utilised for measuring CV, however it failed to get any reasonable graph of the compound due to large conductance.

4.5 Electrosynthesis of amides

A common approach for conducting the electrosynthetic reaction is by using chronocoulommetry (known as bulk electrolysis) where a set charge is required for the reaction to proceed. The reaction is carried out once the voltammetric potential of the compound is chosen and holding the reaction at the said potential. The

equation below is used to calculate the amount of charge required for the electrosynthetic reaction to go to completion:

$$Q = (m_A / RMM)nF$$

Integrating the current during the applied potential step is required to calculate Q (total charge), Q drives the reaction to completion. m_A is the mass (g) of the electroactive analyte, RMM is the relative molecular mass ($gmol^{-1}$), F is the Faraday constant and n is the total number of electrons passed in the electrochemical reaction. The amount of time required for a reaction to go to completion can be calculated by monitoring the charge. To decrease the time taken by a reaction, large surface area electrode and mechanical stirring of the solution are typically employed.

For a Shono oxidation to process only 2 F/mole is required (Scheme 1.6.1). However, excess of 4 F/mole is generally used in literature. Suárez et. al,[16] demonstrated (conversion of **1** to **11** Shono oxidation) the use of varying F/mole and the conversion rate achieved. They showcased that low rates of conversion were achieved when 2 F/mole was used when compared to 4 F/mole. So it was decided 4 F/mole will be utilised when conducting the electrosynthesis.

4.6 Potentiostatic

Once the oxidation potential of the compounds was known, the reaction was carried out on compounds **1** and **5**. There were several downsides to using this method including the amount of time taken to transfer 18 Columbus (6 days). The ^{1}H-NMR of the purified (experimental 6.10) compound after reaction, displayed protons assigned to the electrolyte, leading to conclusion that the product might have decomposed due to the amount of time taken for the reaction to go to completion. No improvements were observed even after changing parameters such as using larger surface area of electrode, conducting the reaction at lower temperature (increases current). As previously mentioned the amount of time it takes for a reaction to complete depends on current, which in this method dropped to approximately 5 mA cm^2 and could not be controlled. The software only allows for one parameter to be selected either oxidation or the current value, as this method required the oxidation potential this increased the amount of time for the reaction.

4.7 Conclusion

As potentiostatic method is time consuming, it will not be used for further electrosynthesis. Chapter 5 will explore another method of electrosynthesis known as galvanostatic where the current is required and not the potential. PDEs as an electrode for organic chemistry will not be explored in the next chapter as the material they are drawn is vulnerable to organic solvents. However, pencil as an electrode will be utilised in the next chapter for electrosynthesis.

Chapter 5 – Galvanostatic method results and Discussion

5.1 Shono-Oxidation

Suárez *et. al*,[16] recently demonstrated the use of Shono oxidation on tertiary amides. They used compound **1** for the electrosynthesis using a potentiostatic method. They also changed numerous other parameters, such as variety of electrolyte. The goal of this research project was to further research the parameter set by Suárez *et. al* [16] and achieve Shono oxidation on a variety of tertiary amides.

As stated in previous chapter, a potentiostatic method was first employed for the electrosynthesis of amides in this research, however it was found to be inadequate in terms of the amount of time taken for the charge (Q) to transfer. Hence an alternative galvanostatic method was selected for the electrosynthesis. Although TBAP is a suitable electrolyte, due to its polarity and non-aqueous solubility, it is difficult to separate the electrolyte from the product by column chromatography. Therefore, an alternative electrolyte of lithium perchlorate was also used.

Optimal current of 20 mA/cm^2 was selected for the galvanostatic method. Currents higher than 20 mA/cm^2 (30, 50 and 100 mA/cm^2) produced discolouration of the electrodes and lead to vigorous heating of the solvents. Currents lower than 20 mA/cm^2 increased the reaction time significantly. Booster module (Autolab Booster20A) was required to produce 100 mA/cm^2, which lead to electrode burn-out and the charge transfer was achieved rapidly. After the experiment where higher currents were used the electrodes were no longer capable of being re-used (the electrode's ability to detect oxidation/reduction was carried out using inner/outer redox probe). The product recovered in the 100 mA/cm^2, 50 mA/cm^2, and 30 mA/cm^2 was mostly starting material, ^{1}H-NMR spectroscopy indicated new peaks forming. Table 5.1.1 highlights the outcomes of the varying currents investigated.
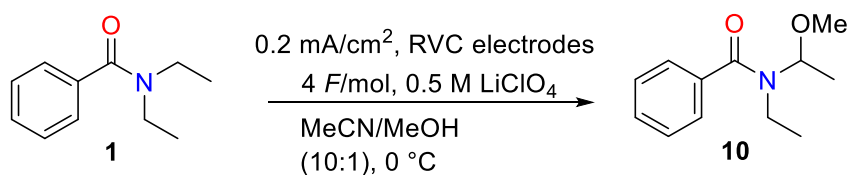

Table 5.1.1. Variation of current at a fixed 4 F/mole on the percentage conversion of the reaction of **1** - **10**. *The remainder was starting material.

| Entry	Current (mA/cm^2)	F/mole	Time (minutes)	Normalised % conversion to 11
1	100	4	2.0	0*
2	50	4	5.0	5*
3	30	4	20.0	10*
4	20	4	90.0	100

The subsections below are divided as followed, the compounds on which Shono oxidation has been achieved, compounds on which dealkylation has occurred, and finally compounds that were unreactive to electrosynthesis. The temperature is kept constant through the whole cell to stop the reaction from overheating (electrolytes are explosive at higher temperature) by stirring and measuring the temperature at interval.

5.2 Shono-oxidised compound
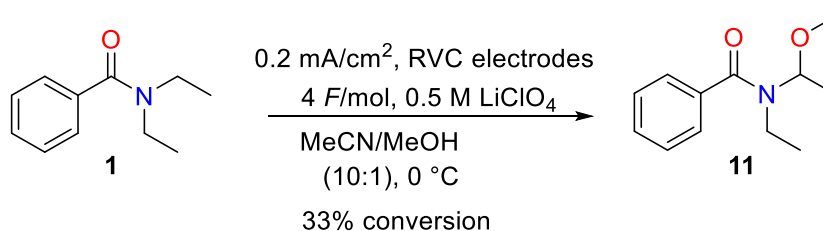
Scheme 5.2.1: Optimised electrosynthesis of **1**.

Shono oxidation (Scheme 5.2.1) of compound **1** takes place when LiClO$_4$ is used as electrolyte. The ^{1}H-NMR of the final compound is compared to the ^{1}H-NMR obtained by Suárez *et.al* [16]. Comparing the synthesise of **1** by Eberson[100] *et.al* via galvanostatic route, it is clear that we have improved the reaction conditions. Eberson[100] *et.al* achieved the same compound using 25 A of current and high surface area graphitic rod, no justification was given for the choice of reaction conditions, the characterisation or the spectra were not reported. This experiment demonstrates that the same end product can be achieved at less current and would not require large surface area graphitic rod.
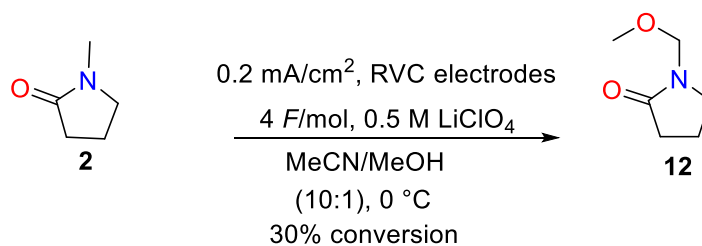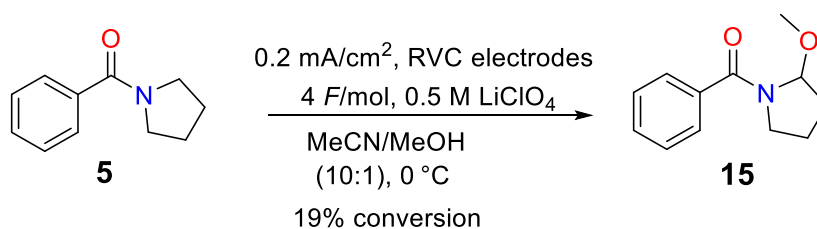
Scheme 5.2.2: Optimised electrosynthesis of **2**.

Compound 2 (Scheme 5.2.2) in LiClO$_4$ produced Shono oxidised product. The ^{1}H-NMR spectrum indicated that although the product had formed, the electrolyte peaks were prominent, even after column chromatography was carried out to separate the electrolyte from the compound.
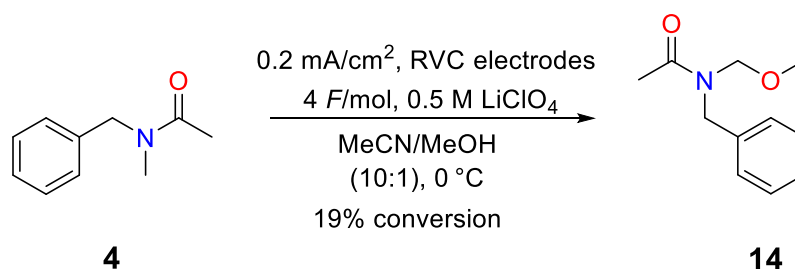
Scheme 5.2.3: Optimised electrosynthesis of **4**.

Shono oxidised product for **4** was recovered when LiClO$_4$ was used as an electrolyte. Isolation proved difficult when TBAP was used as electrolyte for the complex mixture. The ^{1}H-NMR showed that Shono oxidation did not appear to have occurred, the peaks present were assigned to the electrolyte.


Scheme 5.2.4: Optimised electrosynthesis of 4.

Shono-oxidation was observed when compound **5** was electrosynthesised using lithium perchlorate. The ^{1}H-NMR spectrum, obtained of the compound in TBAP although indicated that starting compound had disappeared, however the peak intensities were low (weak product) for analysis.

5.3 Dealkylation of compounds

One of the surprising discoveries that was made during these experiments was the final e-synthesised compound gave a dealkylation product not Shono in several example. Shono oxidation occurs under standard condition; however, in the presence of adventitious water hydroxymethyl species is formed. This has been hypothesised as the cause of dealkylated amine present. This pseudo-electrosynthetic reaction is similar to that performed by endogenous enzymes found in the body such as monoamine oxidase.[103]
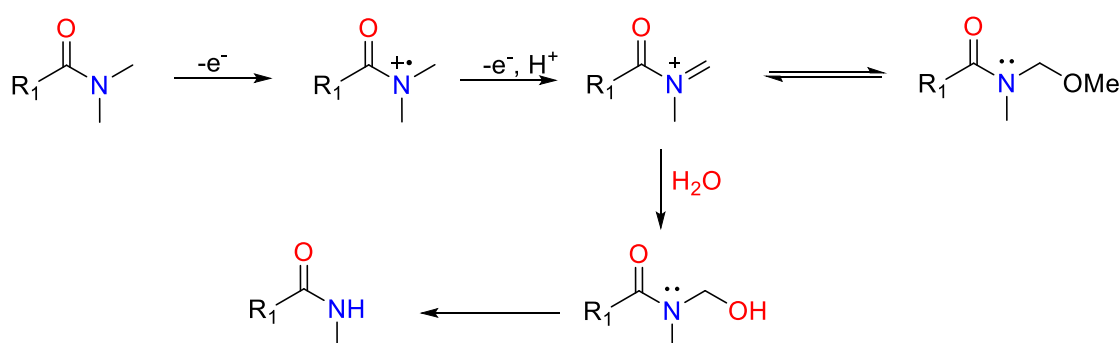

Scheme 5.3.1: Possible reaction mechanism for dealkylation of amides.[104]
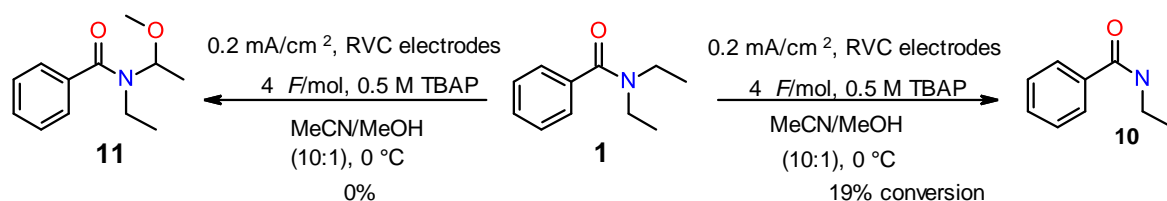
Scheme 5.3.2: Dealkylation of compound **1.**

Under repeated standard conditions, dealkylated amide was produced when TBAP was the source of electrolyte in solution. As the experimental conditions were the same when both TBAP and Lithium perchlorate (LiClO4) were used, the factors that could have affected the outcome are, the amount of coulombs transferred: 2 extra

were transferred than originally required (transferred 22C), this is due to the accuracy of the machine.
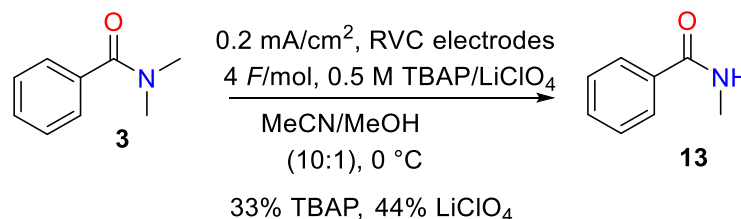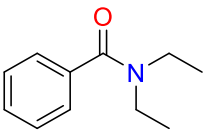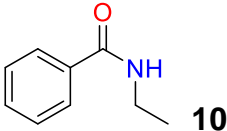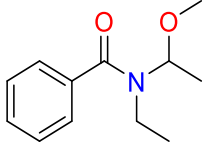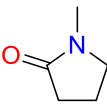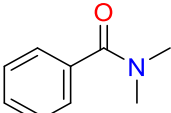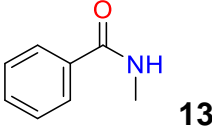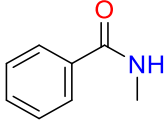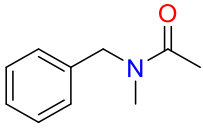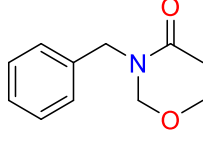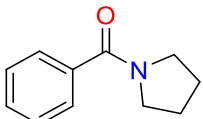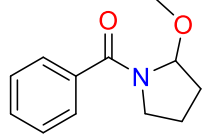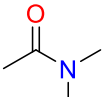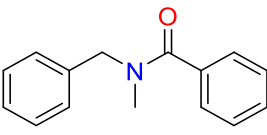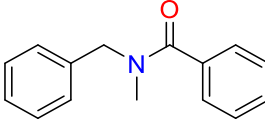

Scheme 5.3.3: Dealkylation of compound **3**.

Dealkylated amide was synthesised when Compound **3** was electrosynthesised with TBAP and lithium perchlorate. Moreover, the solution contained adventitious water (Hanzilk *et al.*[101] also observed adventitious water, when MeOH and MeCN were used as solvent) this factor, coupled with the instability of the methoxy group resulted in the dealkylation of the amide in both instance. (See scheme 5.3.1)

5.5 Unreactive compounds

Shono oxidised product and a dealkylated amine were produced from compound **1** in $LiClO_4$ and TBAP respectively. **2** and **4** indicated formations of Shono oxidation due to the easy access to the C-H activation site and less steric hindrance from the surrounding group. **3** gave a dealkylated compound in both electrolytes; this is due to the two methyl group acting as electron donating groups or possibly due to adventitious water. Compound **5** favoured Shono-oxidised product due to electron-donating group present in the cyclopentane. The carbonyl group is not stabilised by an aryl system, hence making compound **6** less stable. The electrosynthesis in both electrolytes proved difficult to isolate and no starting material was recovered. Compounds **7**, **8** and **9** electrosynthesised using $LiClO_4$ were recov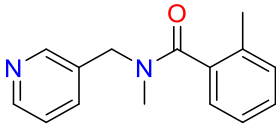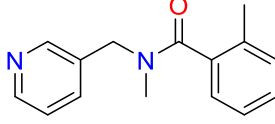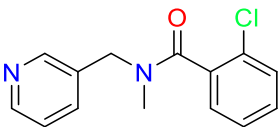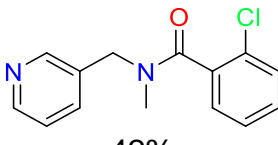ered as the starting products, Shono oxidation or dealkylation did not occur as indicated by the ^{1}H-NMR. **2, 4-9** in TBAP were not determined due to the difficulty of separating electrolyte from the compounds. In summary, the aryl containing analogues are more sterically hindered (because of indirect redox species, i.e. tertiary amides form a radical) and the C-H activation sites becomes more difficult to access as there is interference from the alkyl group on the electrode surface. The overall summary of the electrosynthesised compounds **1- 17** is given below in table 5.5.1.

Entry	Amides	TBAP	LiClO₄
1	Benzoyl N,N-diethyl amide	N-ethylbenzamide **10** 19% isolated	**11** 33% conversion
2	1-methylpyrrolidin-2-one	n.d.	**12** 30% conversion
3	N,N-dimethylbenzamide	N-methylbenzamide **13** 33% isolated	N-methylbenzamide **13** 44% isolated
4	N-benzyl-N-methylacetamide	n.d.	**14** 19% conversion
5	phenyl(pyrrolidin-1-yl)methanone	n.d.	**15** 17% conversion
6	N,N-dimethylacetamide	n.d.	n.d.
7	N-benzyl-N-methylbenzamide	n.d.	44%
8	N-methyl-N-(pyridin-3-ylmethyl)-2-methylbenzamide	n.d.	43%

| 9 | | n.d. | 42% |

Table 5.5.1: Summary of products achieved using Electrosynthesis.

5.6 PDEs and Pencil electrode

Pencil was used as an electrode for synthesising **1**, although it did transfer all the charge required for the electrosynthesis. Once the NMR spectrum of the compound were obtained, no changes were observed and starting material was recovered with a yield of 25%, 75% was lost due to compound decomposition during column chromatography.

5.7 Conclusion

The pencil drawn electrodes are cost effective and easily available in any lab. However, the downside is that they are labour intensive and not reproducible and the substrate on which PDEs are drawn does not support organic solution. Experimental conditions were not changed when using either electrolytes yet compound 1 dealkylated in TBAP.

However, when the experiment was repeated in LiClO$_4$ Shono oxidation took place where as compound 3 dealkylated in both electrolytes. There are several factors that could have affected the experimental outcome such as over oxidation when galvanostatic method was used due to the accuracy of the machine and transferring 2 Columbus over than needed. The solution prepared not being dry enough or the electrolyte playing major role in the synthesis than originally thought. Therefore, in conclusion it has been demonstrated that C-H activation of the bond can be achieved without using chemical oxidations or transition group metals, by using "traceless" electrons. This work also highlighted that dealkylation can take place on a compound, when various electric properties of the compound are considered and finally further test are ongoing to identify the electrosynthesis compound formed in some of the more capricious compounds.

5.8 Future Work

Dealkylation is an important part of the biological process hence naturally the next phase of the project would be exploring how drug like molecules can be dealkylation *via* electrosynthesis. Understand how and why same compounds gives two end product in different electrolyte despite using the same reaction conditions. Investigating how much of an important role the electrolytes play in synthesising the compounds.

Chapter 6 – Experimental Section

6.1 General procedure for cyclic voltammetry of RVC and PDEs

Chemicals were used as received without any additional purification from Sigma-Aldrich and of electrochemical grade. The resistivity of the deionised water used for the preparation of solutions was no less than 18 MΩ cm. Before analysis the solutions were degassed thoroughly with nitrogen. All measurements performed with an Autolab (PGSTAT 100N, The Netherlands) potentiostat/galvanostat with a 10A booster module.

Two types of solutions were used in the experiment. The first solution was an inner-sphere probe and contained 1.0 mM of ammonium iron(II) sulfate hexahydrate and 0.2 M perchloric acid.[64] The second solution was outer-sphere and contained 1.0 mM of hexaammineruthenium(III) chloride and 0.1 M of potassium chloride.[64] Both solutions were prepared in a 100 mL volumetric flask. A typical three electrode system was used where RVC/PDE were used as working electrode and In-house SPE was used as counter and reference electrode [70].

6.2 Fabrication of SPEs

SPEs were fabricated with appropriate stencil designs using a DEK 248 screen-printing machine (DEK, Weymouth, UK).[83] The following material and chemicals were purchased from Gwent Electronic Materials Ltd, UK; carbon-graphite ink formulation, dielectric paste/ink and Ag/AgCl paste. The fabrication method was followed to print the SPEs.[83]

A polyester flexible film (Autostat, 250 µm thickness) was used to screen-print the first layer *via* a previously used carbon-graphite ink formulation.[83] This layer was cured in a fan oven for 30 minutes at 60 °C. By screen-printing Ag/AgCl paste onto the polyester substrate a silver/silver chloride pseudo reference electrode was included into the layer and to cover the connections a dielectric paste/ink was printed onto the layers. The same conditions were used for curing, before the SPE was ready to be used. Screen printed electrodes were then precisely cut to remove the Ag/AgCl pseudo reference and carbon counter and used into a standard three electrodes configuration of electrochemical cell.[83]

6.3 RVC electrodes and dimensions

SPE used had a diameter of 3mm.[70] The surface area of the electrodes was as followed SPE 0.707 mm, RVC (1) 13.6 mm, RVC (2) 175.0 mm, RVC (3) 0.42mm. The pores per inch (PPI) of RVC foam used was RVC (1) 45 PPI, 3% density, RVC (2) 20 PPI and RVC (3) 70 PPI. The scan rate study was conducted using the following scan rates 5 mV/s^{-1}, 10 mV/s^{-1}, 25 mV/s^{-1}, 50 mV/s^{-1}, 100 mV/s^{-1} and 250 mV/s^{-1}.Three electrode system used.

6.4 Scanning microscope images

JEOL JSM-5600LV (JEOL, Tokyo, Japan) model was used to obtain scanning electron microscope (SEM) images.

6.5 PDEs setup and dimensions

The pencil drawn electrodes (PDEs) were fabricated by hand-drawing a 2.0 × 2.0 cm^2 onto A4 printing paper with a thickness of 75 g/m^2 (Lenzing papier, Austria) using a bespoke stainless steel stencil (see Fig. 2).[64] The following commercially available boxes of pencil were used: Derwent, Koh-I-Noor Hardmuth, Linex ® and Castle Art Supplies. The pencil grades used were 2H, H, F, HB, B, 2B, 3B, 4B, 5B, 6B, 7B, 8B and 9B. To complete an area within the 2.0 × 2.0 cm^2 (defined as the working area) is drawn as shown in Figure 6.5.1. This drawn area is referred to 'one draw' within this chapter, this stipulates the pencil is moved while in contact with the substrate such that the complete area is within the 2.0 × 2.0 cm square. A connecting strip was drawn on the top of the square after defining the surface area of working electrode, allowing connection to the potentiostat with crocodile clip.[64] The following draws/layers of the PDEs were investigated: 5 draws, 10 draws, 20 draws, 60 draws and 100 draws the pencils was sharpened after every 15 draws. Three-electrode configuration was utilised. Surface area of PDEs used was 12.0-mm. Surface area of the pencil electrode used (155.0 mm)

Figure 6.5.1: Bespoke metallic stencil (A) used throughout this work to create the PDEs. The PDE after one draw (B). An example of a completed PDE with connecting strip is shown in (C).

6.6 General method for synthesis

All reactions were carried out under nitrogen. Starting materials were used without further purification and purchased from commercial suppliers. The organic layer was dried over MgSO$_4$. Flash silica chromatography (ethyl acetate: petroleum ether, 90:10) was performed using Sigma-Aldrich high-purity grade, pore size 60 Å, 200-400 mesh particle size silica gel. ^{1}H and ^{13}C-NMR spectra were recorded on JEOL ECS 400 MHz NMR spectrometer using TMS as the resonance shift standard. All the chemical shifts (δ) are reported in parts per million and coupling constants (*J*) are reported in Hertz (Hz). Low and High resolution mass spectrometry analysis were obtained using an Agilent 6450 LC-MS/MS system.

6.7 Synthesis of amides

A round bottom flask was charged with a magnetic stirrer bar, acyl chloride (10 mmol), potassium carbonate (2.07 g, 15 mmol), anhydrous tetrahydrofuran (35 mL) and cooled to 0 °C.[96] Under stirring, amine (10 mmol) was added portion wise at 0 °C. The reaction mixture was allowed to stir at room temperature (25° C) for a further 12 h, quenched with hydrochloric acid (1 M, 4 mL) portion-wise and extracted with ethyl acetate (3 × 30 mL), washed with saturated sodium hydrogen carbonate solution (2 × 15 mL) and brine (2 × 15 mL). The solution was concentrated *in vacuo* to afford the title compound. [96]

6.8 General procedures for cyclic voltammetry, potential (v), Fmol^{-1} and electrolyte variation experiments

An undivided glass cell (28 mL) equipped with magnetic stirrer along with rectangular reticulate vitreous carbon anode (4.7 cm^2) and reticulate vitreous carbon cathode (4.7 cm^2).[16] Arranged opposite to one another at a distance of (9.8 mm) with a silver wire reference electrode place (0.4 mm) from the working electrode.[16] To this reaction vessel was added **1-8** (20 mM) in acetonitrilie (9 mL), methanol (0.9 mL) and electrolyte (tetrabutylammonium chloride or lithium perchlorate, 0.5 M). The solution degassed with nitrogen before the CV performed. A blank was carried out (same solution as above with the exception of amide), before scan rate study. Cyclic voltammetry was performed using VerSTAT 3, model 400 (version 2.43.4) potentiostat.

6.9 General procedure for Galvanostatic and Potentiostatic method

For potentiostatic oxidation potential of the compound see table (4.3.1). Typical three electrode system, consisting of rectangular reticulate vitreous carbon anode (4.7 cm^2) and reticulate vitreous carbon cathode (4.7 cm^2), arranged opposite to one another at a distance of (9.8 mm) with a silver wire reference electrode place (0.4 mm) from the working electrode. For galvanostatic 20 mA current was used throughout the experiment, as it was the optimal.

6.10 Electrosynthesis using TBAP

Procedure 6.8 followed for the preparation of reaction mixture. For oxidation potential see table (4.3.1). All measurements were performed with Autolab (PGSTAT 100N, The Netherlands) potentiostat. Once the reaction was completed, column chromatography (ethyl acetate: petroleum ether 0:100 to 20: 80), was carried out to purify the compound to obtain the final compound.

## 6.11 Electrosynthesis using LiClO$_4$

General method 6.8 was followed for preparation of reaction mixture. Reaction carried out in LiClO$_4$, was quenched with sodium sulfite (1.0 M, 4.0 mL) portion-wise and extracted with ethyl acetate (30 mL × 3), washed with saturated sodium hydrogen carbonate solution (15 mL × 2) and brine (15 mL × 2). The organic layer was dried with MgSO$_4$, concentrated *in vacuo* to afford the title compound.

6.12 General procedures for PDEs and pencil electrode

Procedure 6.8 was followed for the preparation of the solution. Pencil drawn electrode was drawn on flexible polyester substrate (Autotex AM, model F157L, 150 μm 122 thickness) at 100 draws. It was used as working electrode with a surface area of 13.0 mm, RVC used as counter and silver wire. For the Pencil electrode, Graphite pencil split into two halves (Figure 3.7) and carved to create a connecting strip, pencil area smoothed surface area of the pencil (155.0 mm).

## 6.13 Characterisation

(1) *N, N- diethylbenzamide*[16]
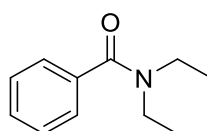
1 (1.60 g, 91%) was afforded as a pale yellow oil. General procedure 6.7 were employed to synthesis the title compound. ^{1}H-NMR (400 MHz, CDCl$_3$): δ ppm 7.46 - 7.30 (m, 5H), 3.53 (br s, 2H, *J*=5.8 Hz), 3.23 (br s, 2H, *J*=5.8 Hz), 1.33 (br s, 3H), 0.97 (br s, 3H);^{13}C NMR (101 MHz, CDCl$_3$) δ ppm 171.4, 137.4, 129.2, 128.5, 126.4, 43.3, 39.3, 14.3, 13.0; Hi-Res LC-MS (ESI) *m/z* calcd for C$_{11}$H$_{15}$NO [M+H$^+$] 178.255, found 178.123. -0.132 ppm difference.
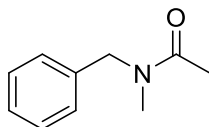
(2) *1-methylpyrrolidin-2-one*
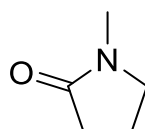
2 purchased amide. ^{1}H-NMR (400 MHz, CDCl$_3$): δ ppm 3.34 (t, 2H), 2.80 (s, 3H) 2.33 (t, 2H), 1.98 (m, 2H).^{13}C NMR (101 MHz, CDCl$_3$): δ ppm 175.1, 49.5, 30.8, 29.6,17.7.

3 *N,N-dimethylbenzamide*[105]
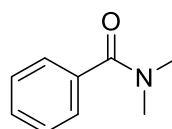
3 purchased amide. ^{1}H-NMR (400 MHz, CDCl$_3$): δ ppm 7.37 (br s, 5H), 3.09 (s, 3H) 2.95 (s, 3H).^{13}C NMR (101 MHz, CDCl$_3$): δ ppm 171.8, 136.4, 1.0, 129.6, 128.4, 128.3, 127.1, 39.7, 35.4.
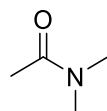
4 *N-Benzyl-N-methylacetamide*[106]

4 (1.40 g, 88%) was afforded as light yellow oil. General procedure 6.6 and 6.7 were employed to synthesis the compound. ^{1}H-NMR (400 MHz, CDCl$_3$): δ ppm 7.41 - 7.11 (m, 5 H), 4.57 (s, 2H, major rotamer), 451 (s, 2H, minor rotamer), 2.92 (s, 3H, minor rotamer), 2.90 (s, 3H major rotamer), 2.14 (s, 3H). ^{13}C NMR (101 MHz, CDCl$_3$): δ ppm 171.3 (m) 170.6 (M), 137.8 (M),137.4 (m),136.4 (m), 129.3, 128.6, 128.2, 127.6, 127.3, 126.2, 54.6 (m), 50.6 (M). 35.8 (M), 22.1 (M), 21.7 (m). Hi-Res LC-MS (ESI) *m/z* calcd for C$_{10}$H$_{13}$NO [M+H$^+$] 164.228, found 164.107. -0.121 ppm difference.

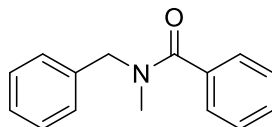**5** *Phenyl(1-pyrrolidinyl) methanone*[107]
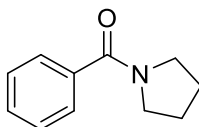
5 (1.40 g, 81%) reaction afforded the title compound as a clear oil. General procedure 6.6 and 6.7 was employed to synthesis the compound. ^{1}H-NMR (400 MHz, CDCl$_3$): δ ppm 7.42 – 7.37 (m, 2H), 7.30 – 7.24 (m, 3H), 3.52 (t, 2H, *J*=6.8 Hz), 3.30 (t, 2H, *J*=6.6 Hz), 1.83 (dd, *J* = 6.5, 13.7 Hz, 2 H), 1.73 (dd, *J* = 13.1, 6.9 Hz, 2 H). ^{13}C NMR (101 MHz, CDCl$_3$): δ ppm 169.8, 137.3, 129.5, 128.6, 127.9, 49.4, 46.2, 26.8, 24.3. Hi-Res LC-MS (ESI) *m/z* calcd for C$_{11}$H$_{13}$NO [M+H$^+$] 176.239, found 176.106. -0.133 ppm difference.

6 *N,N-dimethylacetamide*

6 purchased amide. ^{1}H-NMR (400 MHz, CDCl$_3$): δ ppm 2.95 (s, 3H), 2.87 (s,3H), 2.02 (s, 3H). ^{13}C NMR (101 MHz, CDCl$_3$): δ ppm 170.7, 38.1, 35.2, 21.7.

7 N-Benzyl-N-methylbenzamide

7(1.34 g, 59%) reaction afforded the title compound as a brown-yellow oil. General procedure 6.6 and 6.7 was employed to synthesis the compound. ^{1}H-NMR (400 MHz, CDCl$_3$): δ ppm 7.28 - 7.56 (m, 9H) 7.16 (d, J=6.41 Hz, 1H) 4.75 (br. s., 1H) 4.50 (br. s., 1H), 2.96 (d, 3H); ^{13}C NMR (101 MHz, CDCl$_3$): δ ppm 170.3, 136.3, 135.9, 128. 7, 128.4, 127.6, 126.9, 126.7, 126.0, 50.8, 34.6. Hi-Res LC-MS (ESI) m/z calcd for C$_{15}$H$_{15}$NO [M+H$^+$] 226.229, found 226.123, -0.106 ppm difference.

8 N,2-Dimethyl-N-(3-pyridinylmethyl) benzamide
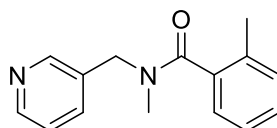

8 (0.73 g, 47%) reaction afforded the title compound as a brown-yellow oil.^{1}H-NMR (400 MHz, CDCl$_3$): δ ppm 8.45 - 8.70 (m, 2H) 7.68 - 7.87 (m, 1H) 7.38 - 7.55 (m, 1 H) 7.09 - 7.38 (m, 6H) 4.77 (br. s., 2H) 2.66 - 2.75 (m, 3H) 2.23 - 2.33 (m, 3H); ^{13}C NMR (101 MHz, CDCl$_3$): δ ppm 168.4, 149.2 148.4,136.6,135.0,131.9,130.2, 129.5, 129.2, 128.6,126.5, 123.6, 52.1, 35.6, 19.02. Hi-Res LC-MS (ESI) m/z calcd for C$_{15}$H$_{16}$N$_2$O [M+H$^+$] 241.314, found 241.138. -0.176 ppm difference.

9 2-chloro-N-Methyl-N-(3-pyridinylmethyl) benzamide
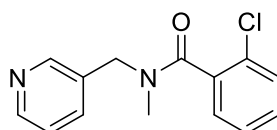
9 (0.82 g, 78%) reaction afforded the title compound as a yellow oil. ^{1}H-NMR (400 MHz, CDCl$_3$): δ ppm 8.50 - 8.70 (m, 2H) 7.76 - 7.86 (dt, 1H) 7.31 - 7.58 (m, 5H) 4.28 - 5.14 (d, 2H) 2.68 - 3.12 (d, 3H); ^{13}C NMR (101 MHz, CDCl$_3$): δ ppm 168.9, 149.1, 147.4, 136.2, 135.1, 131.0, 129.6, 129.1, 128.2, 126.6, 123.7, 51.3, 35.7; Hi-Res LC-MS (ESI) m/z calcd for C$_{14}$H$_{13}$N$_2$OCl [M+H$^+$] 261.729, found 261.007. -0.722 ppm difference.

10 *N*-ethylbenzamide[108]
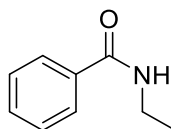
10 (10 mg, 33%) was afforded as pale yellow oil. General method 6.9 and 6.10 employed for the e-synthesis. ^{1}H-NMR (400 MHz, CDCl$_3$): δ ppm 7.39-7.75 (m, 5H), 6.06 (br s, 1H), 3.53-3.46 (m, 2H), 1.25 (t, *J* = 7.2 Hz, 3 H).

11 *N*-ethyl-*N*-(1-methoxyethyl) benzamide[16]
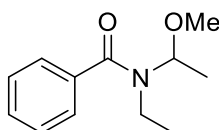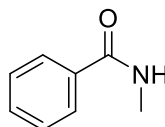

11 (8 mg, 19%) was afforded as pale yellow oil. General method 6.9 and 6.11 used for synthesising the compound. Reaction carried out in LiClO$_4$, gives us Shono oxidised product. ^{1}H-NMR (400 MHz, CDCl$_3$): δ ppm 7.84-7.27 (m, 5H) 4.84 (s,1H) 3.69(s, 0.85H) 3.53-3.41 (m, 1.5H) 3.05 (s., 3H) 1.37 (d, *J*=6.41 Hz, 3H) 1.30 - 1.18 (m, 3H).

13 *N-methylbenzamide*[109]

13 (12 mg, 44%) was afforded as colourless oil in electrolyte LiClO$_4$. General method 6.9, 6.10 and 6.11 were used for synthesising the compound. ^{1}H-NMR (400 MHz, CDCl$_3$): δ ppm 7.74 (d, *J* = 7.3 Hz, 2 H), 7.48 - 7.43 (m, 1 H), 7.42 - 7.37 (m, 2 H), 6.29 (br. s., 1 H), 2.99 (d, *J* = 4.5 Hz, 3 H).

Reference

1. B. A. Frontana-Uribe, R. D. Little, J. G. Ibanez, A. Palma and R. VasquezMedrano, *Green Chem.,* 2010, **12**, 2099-2119.

2. S. L. James, C. J. Adams, C. Bolm, D. Braga, P. Collier, T. Friščić, F. Grepioni, K. D. M. Harris, G. Hyett, W. Jones, A. Krebs, J. Mack, L. Maini, A. G. Orpen, I. P. Parkin, W. C. Shearouse, J. W. Steed and D. C. Waddell, *Chem. Soc. Rev.,* 2012, **41**, 413-447.

3. E. O'Reilly and N. J. Turner, *Nat. Chem. Biol.*, 2013, **9**, 285-288.

4. C. K. Prier, D. A. Rankic, D. W. C MacMillan, *Chem. Rev.,* 2013, **113**, 5322−5363.

5. K. D. Moeller, *Tetrahedron*, 2000, **56**, 9527−9554.

6. J. B. Sperry and D. L. Wright, *Chem. Soc. Rev.,* 2006, **35**, 605−621.

7. C. A. C Sequeira and D. M. F Santos, J. Braz. *Chem. Soc.,* 2009, **20**, 387−406.

8. J. Yoshida, K. Kataoka, R. Horcajada, A. Nagaki, *Chem. Rev.,* 2008, **108**, 2265−2299.

9. Y. N. Ogibin, M. N. Elinson and G. I. Nikishin, Russ. *Chem. Rev.,* 2009, **78**, 89−140.

10. M. C. Bryan, B. Dillon, L. G. Hamann, G. J. Hughes, M. E. Kopach, E. A. Peterson, M. Pourashraf, I. Raheem, P. Richardson, D. Richter and H.F. Sneddon, *J. Med. Chem.,* 2013, **56**, 6007−6021.

11. T. Cernak, K. D. Dykstra, S. Tyagarajan, P. Vachal and S. W. Krska, Chem. Soc. Rev., 2016, **45**, 546−576.

12. C. A. Kuttruff, M. D. Eastgate and P. S. Baran, Nat. Prod. Rep., 2014, **31**, 419−432.

13. T. F. O'Brien, T. V. Bommoraju and F. Hine, Handbook of Chlor-Alkali Technology; Springer: Dordecht, Netherlands, 2005.

14. E. J. Horn, B. R. Rosen, and P.S. Baran, *ACS Cent. Sci.,* 2016, **2**, 302-308.

15. D. Pletcher, A First Course in Electrode Processes, The Electrochemical Consultancy, U.K., 1991.

16. P. Alfonso-Suárez, A. V. Kolliopoulos, J. P. Smith, C. E. Banks and A. M. Jones, *Tetrahedron Lett.,* 2015, **56**, 6863-6867.

17. B. R. Rosen, E. W. Werner, A. G. O'Brien and P. S. Baran, *J. Am. Chem. Soc.,* 2014, **136**, 5571-5574.

18. H. Ding, P. L. DeRoy, C. Perreault, A. Larivee, A. Siddiqui, C. G. Caldwell, S. Harran and P. G. Harran, *Angew. Chem. Int. Ed.,* 2015, **54**, 4818−4822.

19. K. J. Frankowski, R. Liu, G. L. Milligan, K. D. Moeller, and J. Aube, *Angew. chem. Int. Ed.,* 2015, **54**, 1055.

20. (a) J. M. Humphrey and A. R. Chamberlin, *Chem. Rev.*, 1997, **97**, 2243-2266; (b) J. W. Bode, Curr. Opin. *Drug Discov. Dev.,* 2006, **9**, 765-775; (c) T. Cupido, J. Tulla- Puche, J. Spengler and F. Albericio, *Curr. Opin. Drug Discov. Dev.,* 2007, **10**, 768-783; (d) G. Wang, T. Yuan and D. Li, *Angew. Chem., Int. Ed.,* 2011, **50**, 1380-1383; (e) X. Zhang, W. T. Teo and P. W. H. Chan, *J. Organomet. Chem.,* 2011, **696**, 331-337.

21. T. Cupido, J. Tulla-Puche, J. Spengler and F. Albericio, *Curr. Opin. Drug Discovery Dev.*, 2007, **10**, 768-783; b) J. W. Bode, *Curr. Opin. Drug Discovery Dev.,* 2006, **9**, 765-775; c) J. M. Humphrey, A. R. Chamberlin, *Chem. Rev.,*1997, **97**, 2243-2267.

22. F. Renzhong, Y. Yang, C. Zhikai, L. Wenchen, M. Yongfeng, W. Quan, Y. Rongxin, *Tetrahedron*, 2014, **70**, 9492-9499.

23. J. B. Sperry and D. L. Wright, *Chem. Soc. Rev.,* 2006, **35**, 605-621.

24. E. Steckhan, Topics in current chemistry. Electrochemistry, Vol.3, Springer, NY, 1988.

25. B. Speiser, in Encyclopedia of Electrochemistry, ed. A. J. Bard and M. Stratmann, H. J. Schafer, Wiley-VCH, Germany, 2004, vol. 8, chap. 1.

26. R. D. Little and K. D. Moeller, *Interface.,* 2002, **11**, 36–42; (b) F. Tang, C. Chen and K. D. Moeller, *Synthesis.,* 2007, 3411–3420.

27. J. I. Yoshida, *Chem. Commun.,* 2005, **36**, 4509–4516.

28. H. Lund and O. Hammerich, Organic Electrochemistry, Marcel Dekker Inc, USA, 2001.

29. F. Scholz, C. J. Pickett, Encyclopedia of Electrochemistry, ed. A. J. Bard and M. Stratmann, F. Scholz, C. J. Pickett, Wiley-VCH, Germany, 2004, vol. 7.

30. C. A. Paddon, G. J. Pritchard, T. Thiemann and F. Marken, *Electrochem. Commun.,* 2002, **4**, 825–831.

31. D. Horii, M. Atobe, T. Fuchigami and F. Marken, *J. Electrochem. Soc.,* 2006, **153**, D143– D147.

32. P. He, P. Watts, F. Marken and S. J. Haswell, *Lab Chip*, 2007, **7**, 141–143.

33. A. Nagaki, M. Togai, S. Suga, N. Aoki, K. Mae and J.-I. Yoshida, *J. Am. Chem. Soc.,* 2005, **127**, 11666–11675.

34. (a) A. Redden, R. J. Perkins and K. D. Moeller, *Angew. Chem., Int. Ed.*, 2013, **52**, 12865−12868; (b) J. A. Smith and K. D. Moeller, *Org. Lett.,* 2013, **15**, 5818−5821; (c) A. Redden and K. D. Moeller, *Org. Lett.*, 2011, **13**, 1678−1681; (d) H. C. Xu and K. D. Moeller, *Angew. Chem., Int. Ed.* 2010, **49**, 8004−8007; (e) G. Xu and K. D. Moeller, *Org. Lett.,* 2010, **12**, 2590−2593; (f) H. C. Xu and K. D. Moeller, *Org. Lett.,* 2010, **12**, 1720−1723.

35. (a) H. C. Xu and K. D. Moeller, *J. Am. Chem. Soc.,* 2010, **132**, 2839−2844; (b) H. C. Xu and K. D. Moeller, *J. Am. Chem. Soc.,* 2008, **130**, 13542−13543. (c) H. Wu and K. D. Moeller, *Org. Lett.,* 2007, **9**, 4599−4602; (d) F. Tang and K. D. Moeller, *J. Am. Chem. Soc.*, 2007, **129**, 12414−12415; (e) J. D. Brandt and K. D. Moeller, *Org. Lett.,* 2005, **7**, 3553−3556; (f) Y. T. Huang and K. D. Moeller, *Org. Lett.,* 2004, **6**, 4199−4202.

36. (a) J. Mihelcic and K. D. Moeller, *J. Am. Chem. Soc.*, 2004, **126**, 9106−9111; (b) J. Mihelcic and K. D Moeller, *J. Am. Chem. Soc.,* 2003, **125**, 36−37; (c) S. Q. Duan and K. D. Moeller, *J. Am. Chem. Soc.,* 2002, **124**, 9368−9369; (d) A. Sutterer and K. D. Moeller,*J. Am. Chem. Soc.*, 2000, **122**, 5636−5637; (e) D. A. Frey, S. H. K. Reddy and K. D. Moeller, *J. Org. Chem.*, 1999, **64**, 2805−2813; (f) D. A. Frey, N. Wu and K. D. Moeller, *Tetrahedron Lett.,*1996, **37**, 8317−8320.

37. (a) J. B. Sperry, I. Ghiviriga and D. L. Wright, *Chem. Commun.,* 2006, **35**, 194−196; (b) J. B. Sperry and D. L. Wright, *J. Am. Chem. Soc.,* 2005, **127**, 8034−8035; (c) J. B. Sperry and D. L. Wright, *Tetrahedron Lett.,* 2006, **62**, 6551−6557.

38. (a) J. B. Sperry, C. R. Whitehead, I. Ghiviriga, R. M. Walczak and D. L. Wright, *J. Org. Chem.,* 2004, **69**, 3726−3734; (b) J. B. Sperry and D. L. Wright, *Tetrahedron Lett.,* 2005, **46**, 411−414; (c) C. R. Whitehead, E. H. Sessions, I. Ghiviriga and D. L. Wright, *Org. Lett.,* 2002, **4**, 3763−3765.

39. A. W. G. Burgett, Q. Li, Q. Wei and P. G. Harran, *Angew. Chem., Int. Ed.,* 2003, **42**, 4961−4966.

40. (a) C. Gutz, M. Selt, M. Banziger, C. Bucher, C. Romelt, N. Hecken, F. Gallou, T. R. Galvao and S. R. Waldvogel, *Chem. Eur. J.,* 2015, **21**, 13878−13882;

(b) C. Gutz, M. Banziger, C. Bucher, T. R. Galvao and S. R. Waldvogel, *S. Org. Process Res. Dev.*, 2015, **19**, 1428−1433.

41. B. H. Nguyen, R. J. Perkins, J. A. Smith and K. D. Moeller, *J. Org. Chem.,* 2015, **80**, 11953-11962.

42. D. T. Rensing, B. H. Nguyen and K. D. Moeller, *Org. Chem. Front.,* 2016, **3**, 1236-1240.

43. R. Hayashi, A. Shimizu and J. Yoshida, *J. Am. Chem. Soc.,* 2016, **138**, 8400-8403.

44. E. J. Horn, B. R. Rosen, Y. Chen, J. Tang, K. Chen, M. D. Eastgate and P. S. Baran, *Nature,*2016, **533**, 78-81.

45. P. M. Killoran, S. B. Rossington, J. A. Wilkinson and J. A. Hadfield, *Tetrahedron Lett.,* 2016, **57**, 3954-3957.

46. T. Shono, H. Hamaguchi and Y. Matsumura, *J. Am. Chem. Soc.,* 1975, **97**, 4264-4268.

47. T. Shono, Y. Matsumura, K. Tsubata, *J. Am. Chem. Soc.,* 1981, **103**,1172–1176.

48. J. Yoshida, Kazuhide, K. Kataoka, R. Horajada and A. Nagaki, *Chem. Rev.,*2008, **108**, 2265-2299.

49. A. M. Jones and C. E. Banks, Beilstein *J. Org. Chem.,* 2014, **10**, 3056-3072.

50. M. A. Kabeshov, B. Musio, P. R. D. Murray, D. L. Browne, S. V. Ley., *Org. Lett.,* 2014, **16**, 4618–4621.

51. J. C. Lewis, B. Redfern, F. C. Cowlard, *Solid-State Electronics.,*1963, **6**, 251–254.

52. F. C. Cowlard, J. C. Lewis, Am. J. Mater. Sci. Eng., 1976, **2**, 507–510.

53. J. M. Friedrich, C. P-de-León, G. W. Reade and F. C. Walsh, *J. Electroanal. Chem.,* 2004, **561**, 203-217.

54. G. K. Chandler, J. D. Genders and D. Pletcher, *Platinum Met. Rev.,* 1997, **21**, 54-63.

55. A. Tentorino, U. Casolo-Ginelli, *J. Appl. Electrochem.,* 1978, **8**, 195.

56. J. Wang, *Electrochim. Acta.,* 1981, **26**, 1721.

57. M.G. Wickham, P.H. Cleveland, P.S. Binder, P.H. Akers, *Ophthalmic Res.*, 1983, **15**, 116-120.

58. M. Mastragostino, S. Valcher, *Electrochim. Acta.,* 1983, **28**, 501-505.

59. U. Fischer, R. Saliger, V. Bock, R. Petricevic and J. Fricke, *J. Porous Mater.,* 1997, **4**, 281-285.

60. W. C. Moss, *Appl. Therm. Eng.,* 1998,**18**, XXIV.

61. D. Szanto, P. Trinidad, F.C. Walsh, *J. Appl. Electrochem.,* 1998, **28**, 251-258.

62. W.J. Blaedel, J. Wang, *Anal. Chem.,*1980, **52**, 1697-1700.

63. G.W. Reade, PhD Thesis, University of Portsmouth, UK, 1996.

64. J. Wang and H. Dewald, *Anal. Chim. Acta.,*1982, **136**, 77-84.

65. P. A. Flowers, M. A. Maynor and D. E. Owens, *Anal. Chem.,* 2002, **74**, 720.

66. M. A. Lange and J. Q. Chambers, *Anal. Chim. Acta.,*1989, **175**, 89.

67. R. G. Compton, C. E. Banks, Understanding voltammetry, ICP, London, 2011.

68. A. J. Fry, Synthetic Organic Electrochemistry., Harper & Row, USA, 1972.

69. R. S. Nicholson, *Anal. Chem.,*1965, **37**, 1351–1355.

70. C. W. Foster, D. A. C. Brownson, AP. R. D. Souza, E. Bernalte, J. Iniesta, Bertotti, M. Bertotti and C. E. Banks, *Analyst.,* 2016, **141**, 4055-4064.

71. D. A. C. Brownson, S. A. Varey, F. Hussain, S. J. Haigh and C. E. Banks, *Nanosacle.*, 2014, **6**, 1607-1621.

72. J. P. Metters, S. M. Houssein, D. K. Kampouris and C. E. Banks, *Anal. Methods.,* 2013, **5**, 103–110.

73. I. Lavagnini, R. Antiochia and F. Magno, *Electroanalysis*, 2004, **16**, 505–506.

74. C. E. Banks, R. G. Compton, A. C. Fisher and I. E. Henley, *Phys. Chem. Chem. Phys.,* 2004, **6**, 3147–3152.

75. Y. S. Grewal, M. J. A. Shiddiky, S. A. Gray, K. M. Weigel, G. A. Cangelosi and M. Trau, *Chem. Commun.,* 2013, **49**, 1551–1553.

76. L. R. Cumba, C. W. Foster, D. A. C. Brownson, J. P. Smith, J. Iniesta, B. Thakur, D. R. do Carmoa and C. E. Banks, *Analyst.,* 2016, **141**, 2791-2799.

77. D. A.C. Brownson, D. K. Kampouris and C. E. Banks, *Chem. Soc. Rev.,* 2012, **41**, 6944–6976.

78. P. Chen and R.L. McCreery, *Anal. Chem.,* 1996, **68**, 3958-3965.

79. M. R. Kagan and R. L. McCreery, *Langmuir.,* 1995, **11**, 4041-4047.

80. W. Li, C. Tan, M. A. Lowe, H. D. Abruna and D. C. Ralph, *ACS Nano.,* 2011, **5**, 2264-2270.

81. A. Chou, T. Bocking, N. K. Singh, and J. J. Gooding, *Chem. Commun.,* 2005, **7**, 842–844.

82. T. S. Miller, N. Ebejer, A. G. Gueell, J. V. Macpherson and P. R. Unwin, *Chem. Commun.,* 2012, **48**, 7435–7437.

83. W. Yuan, Y. Zhou, Y. Li, C. Li, H. Peng, J. Zhang, Z. Liu, L. Dai and G. Shi, *Sci. Rep.*, 2013, **3**, 2248.

84. K. K. Cline, M.T. McDermott and R.L. McCreery, *J. Phys. Chem.,* 1994, **98**, 5314–5319.

85. R. J. Bowling, R. T. Packard and R. L. McCreery, *J. Am. Chem. Soc.,* 1989, **111**, 1217–1223.

86. D. A. C. Brownson, S. A. Varey, F. Hussain, S. J. Haigh and C. E. Banks, *Nanoscale*, 2014, **6**, 1607–1621.

87. D. A. C. Brownson and C. E. Banks, *Electrochem. Commun.,* 2011, **13**, 111–113.

88. W. Li, C. Tan, M. A. Lowe, H. D. Abruña and D. C. Ralph, *ACS Nano.,* 2011, **5**, 2264–2270.

89. E. Bernalte, C. W. Foster, D. A. C. Brownson, M. Mosna, G. C. Smith and C. E. Banks, *Biosensors.,* 2016, **6**, 45.

90. L. C. S. Figueiredo-Filho, D. A. C. Brownson, O. Fatibello-Filho and C. E. Banks, *Analyst.,* 2013, **138**, 4436–4442.

91. J. P. Metters, R. O. Kadara and C. E. Banks, *Analyst.,* 2011, **136**, 1067-1076.

92. K. C. Honeychurch, *Anal. Methods.,* 2015, **7**, 2437–2443.

93. J. P. Hart and S. A. Wring, *Electroanalysis.,* 1994, **6**, 617-624.

94. K. C. Honeychurch and J. P. Hart, *TrAC.,* 2003, **22**, 456-469.

95. D. King, J. Friend and J. Kariuki, *J. Chem. Educ.,* 2010, **87**, 507–509.

96. E. Alipour and S. Gasemlou, *Anal. Methods.,* 2012, **4**, 2962–2969.

97. N. Dossi, R. Toniolo, F. Impellizzieri and G. Bontempelli, *J. Electroanal. Chem*., 2014, **722–723**, 90–94.

98. N. Dossi, R. Toniolo, A. Pizzariello, F. Impellizzieri, E. Piccin and G. Bontempelli, *Electrophoresis.,* 2013, **34**, 2085–2091.

99. N. Dossi, R. Toniolo, F. Terzi, F. Impellizzieri and G. Bontempelli, *Electrochim. Acta.,* 2014, **146,** 518–524.

100. N. Dossi, R. Toniolo, E. Piccin, S. Susmel, A. Pizzariello and G. Bontempelli, *Electroanalysis.,* 2013, **25**, 2515–2522.

101. L. Eberson, J. Hlavaty, L. Jönsson, K. Nyberg, R. Servin, H. Sternerup and L. G. Wistrand, *Acta Chem. Scand. B.,* 1979, **33**, 113–115.

102. J. Clayden, N. Greeves and S. Warren, Organic chemistry, OUP, Oxford, 2012.

103. J. Kirchmair, M. J. Williamson, A. M. Afzal, J. D. Tyzack, A. P. K. Choy, A. Howlett, P. Rydberg and R. C. Glen, *J. Chem. Inf. Model.,* 2013, **53**, 2896-2907.

104. L. R. Hall, R. T. Iwamoto and R. P. Hanzlik, *J. Org. Chem.,* 1989, **54**, 2446-2451.

105. L. Zhang, W. Wang, A. Wang, Y. Cui, X. Yang, Y. Huang, X. Liu, W. Liu, J. Y. Son, H. Oji and T. Zang, Green Chem., 2013, **15**, 2680-2684.

106. T. B. Nguyen, J. Sorres, M. Q. Tran, L. Ermolenko and A. Mourabit, *Org. Lett.,* 2012, **14**, 3202-3205.

107. R. S. Mane, T. Sasaki and B. M. Bhanage, *RSC Adv.,* 2015, **5**, 94776-94785.

108. M. Arefi, D. Saberi, M. Karimi and A. Heydar, *ACS Comb. Sci.,* 2015, **17**, 341347.

109. H. Huang, G. Yuan, X. Li, H. Jiang, *Tetrahedron Lett.,* 2013, **54**, 7156-7159.

Supplementary material
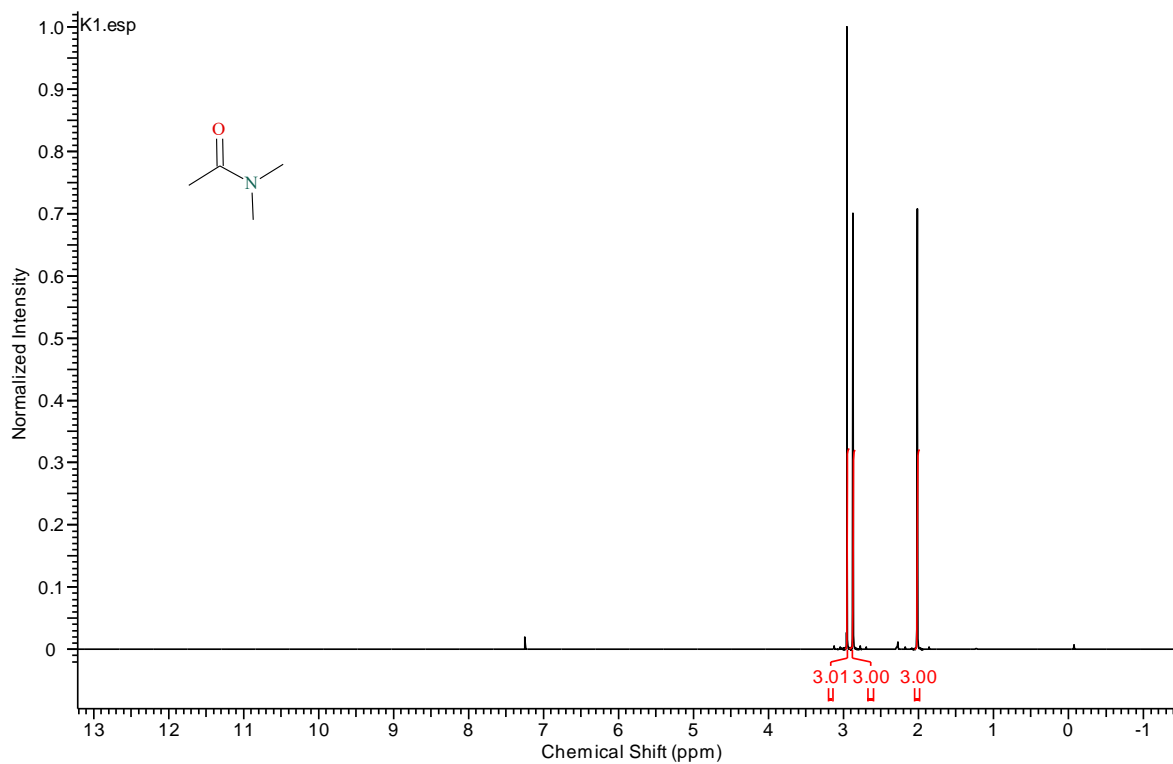## ¹H-NMR spectra of compounds prepared
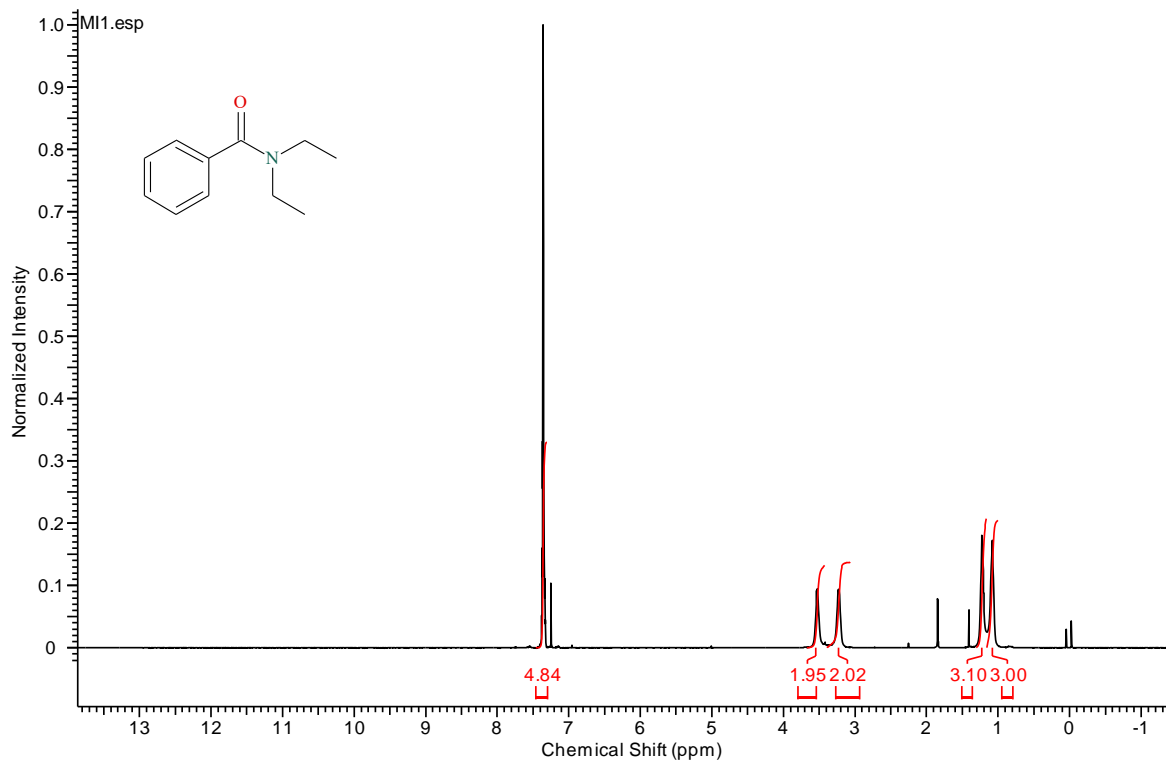
¹H-NMR spectra of **1** (400MHz, CDCl₃)
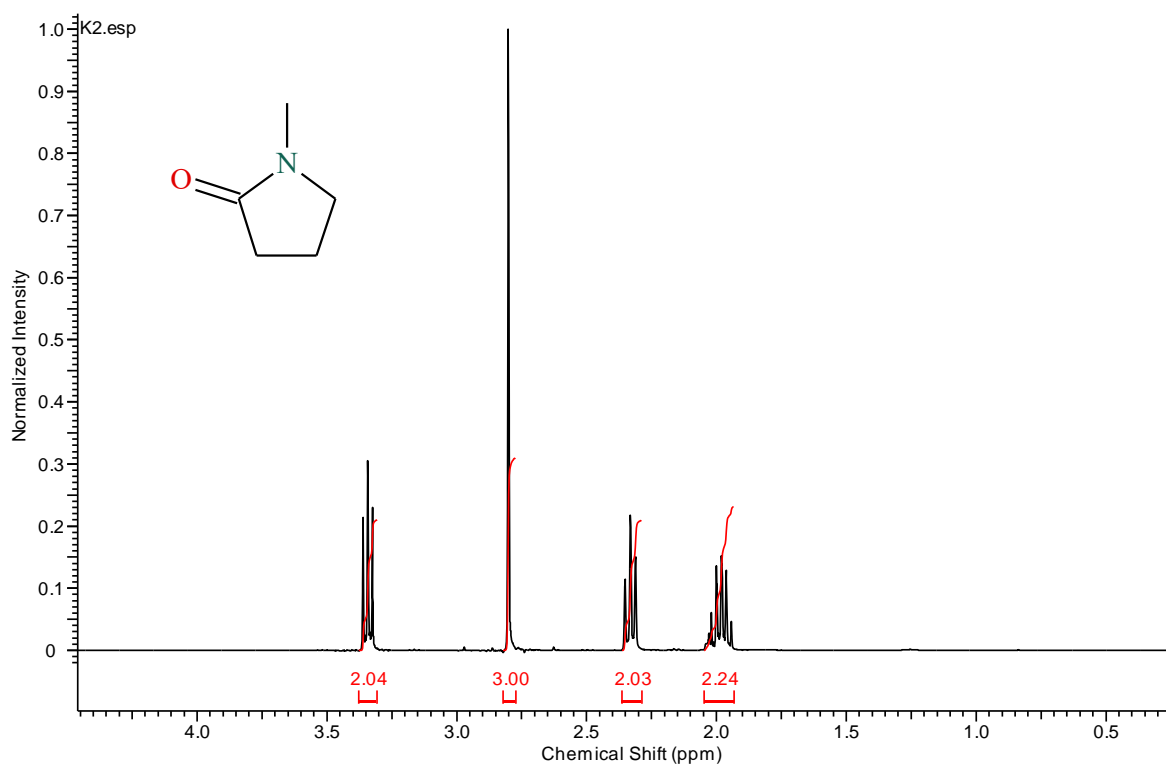
¹H-NMR spectra of **2** (400MHz, CDCl₃)
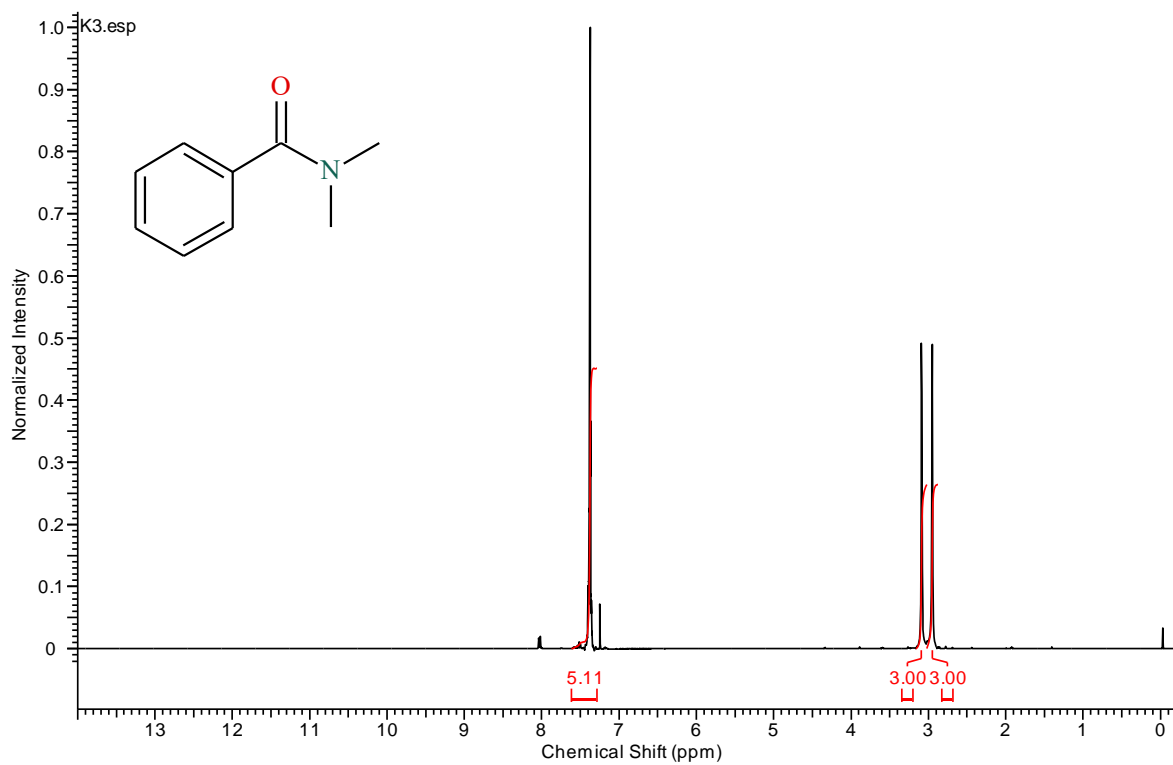
^{1}H-NMR spectra of **3** (400MHz, CDCl$_3$)
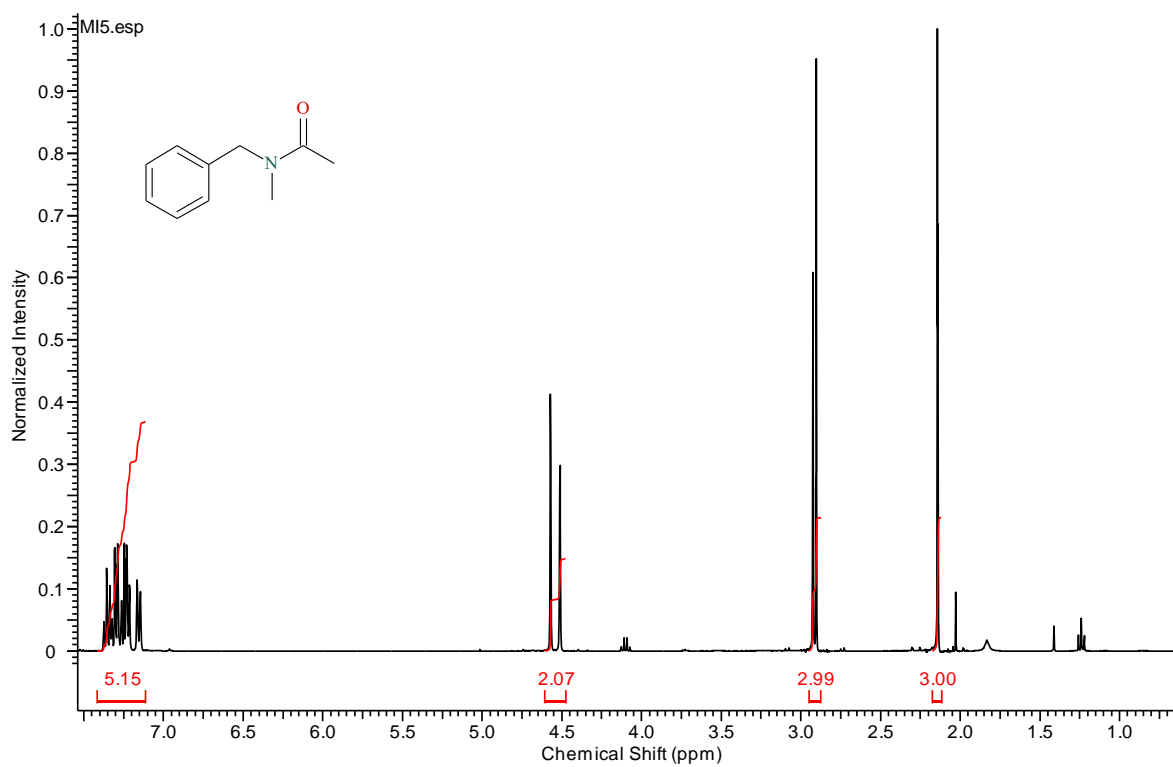
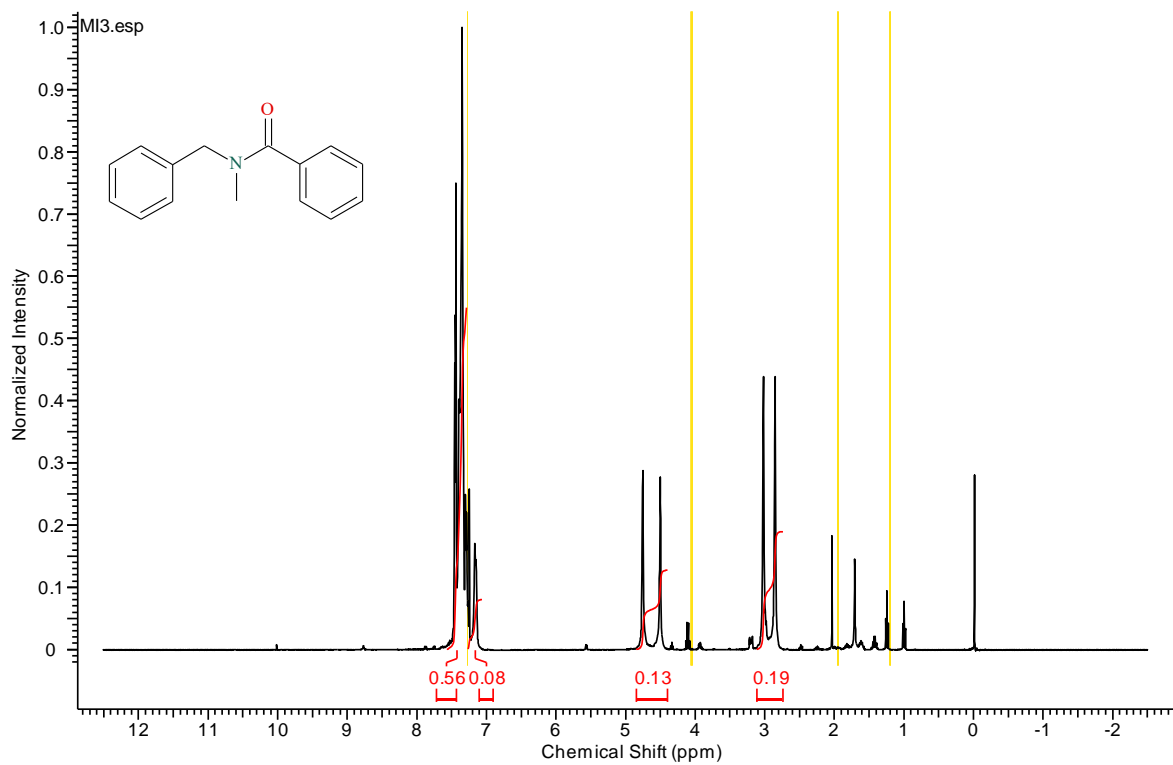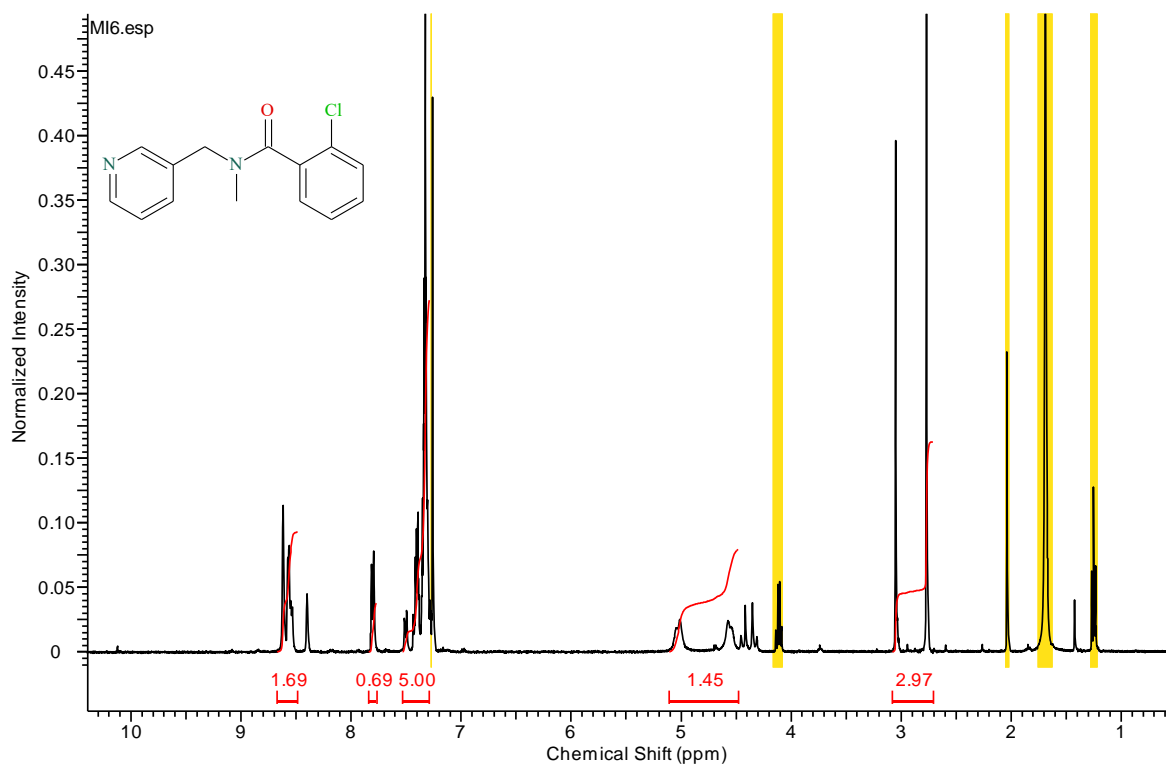^{1}H-NMR spectra of **4** (400MHz, CDCl$_3$)
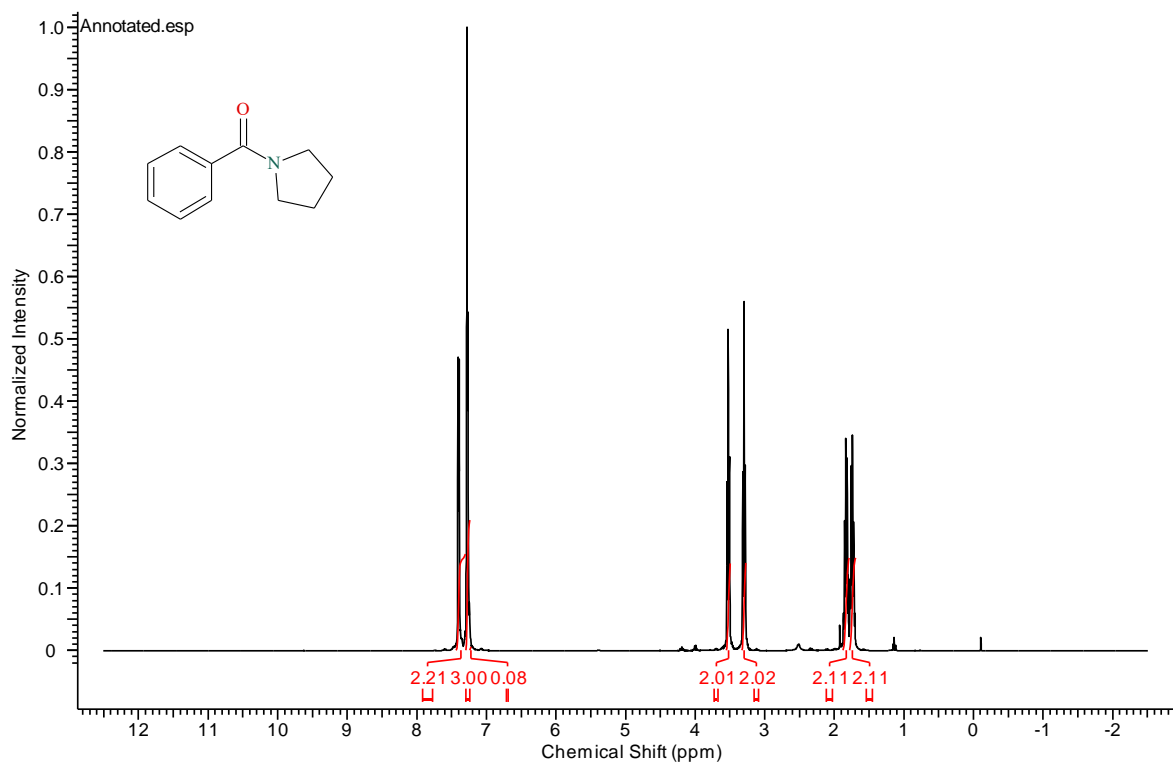
^{1}H-NMR spectra of **5** (400MHz, CDCl$_3$)

^{1}H-NMR spectra of **6** (400MHz, CDCl$_3$)

^{1}H-NMR spectra of **7** (400MHz, CDCl$_3$)
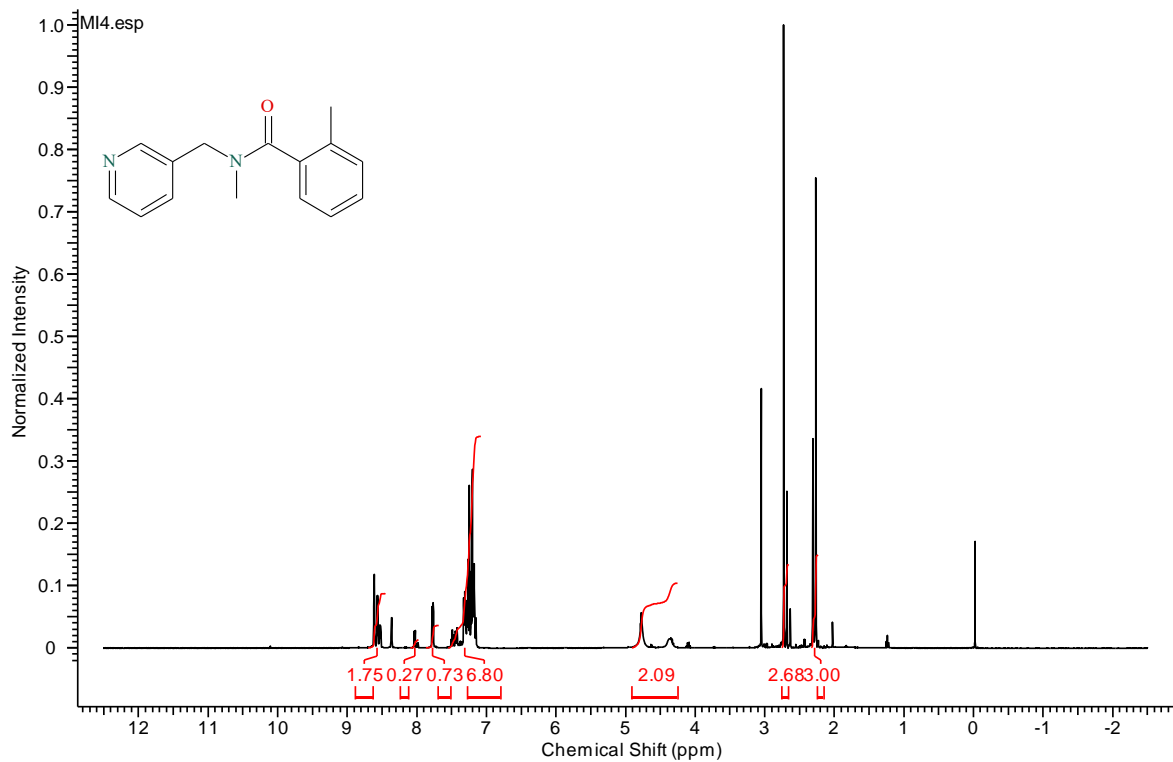
^{1}H-NMR spectra of **8** (400MHz, CDCl$_3$)

^{1}H-NMR spectra of **9** (400MHz, CDCl$_3$)
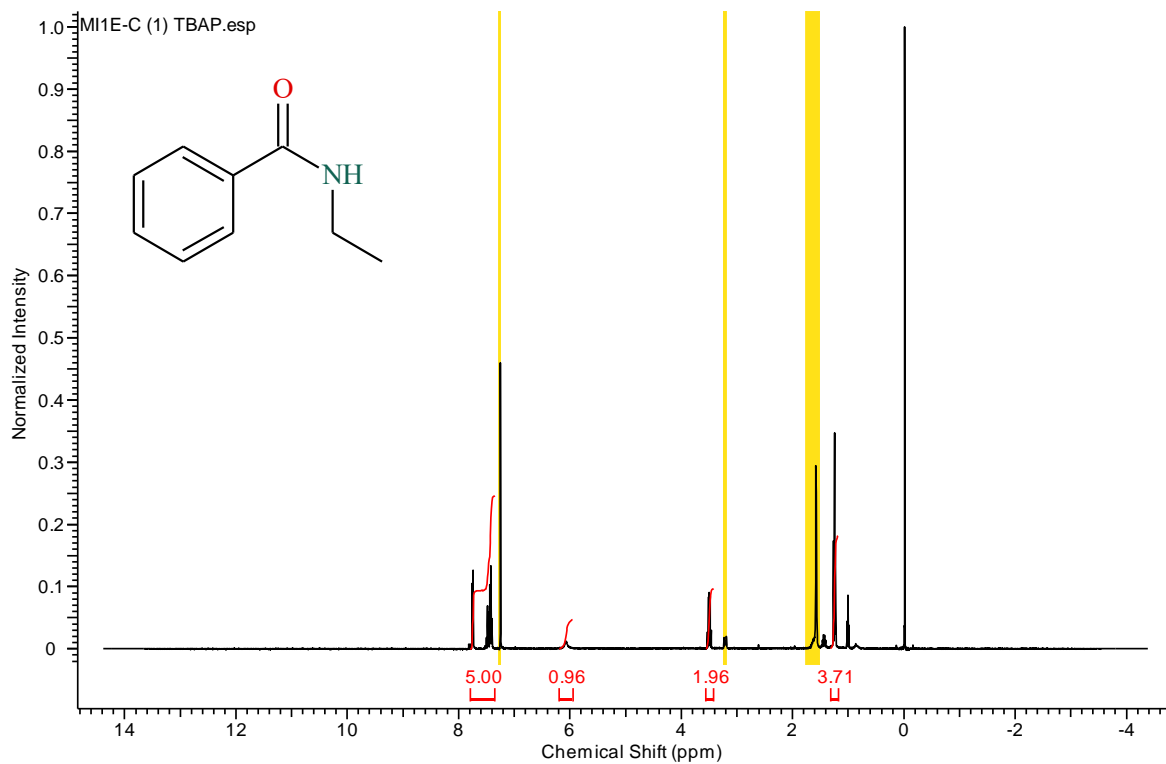
^{1}H-NMR spectra of **10** (400MHz, CDCl$_3$)
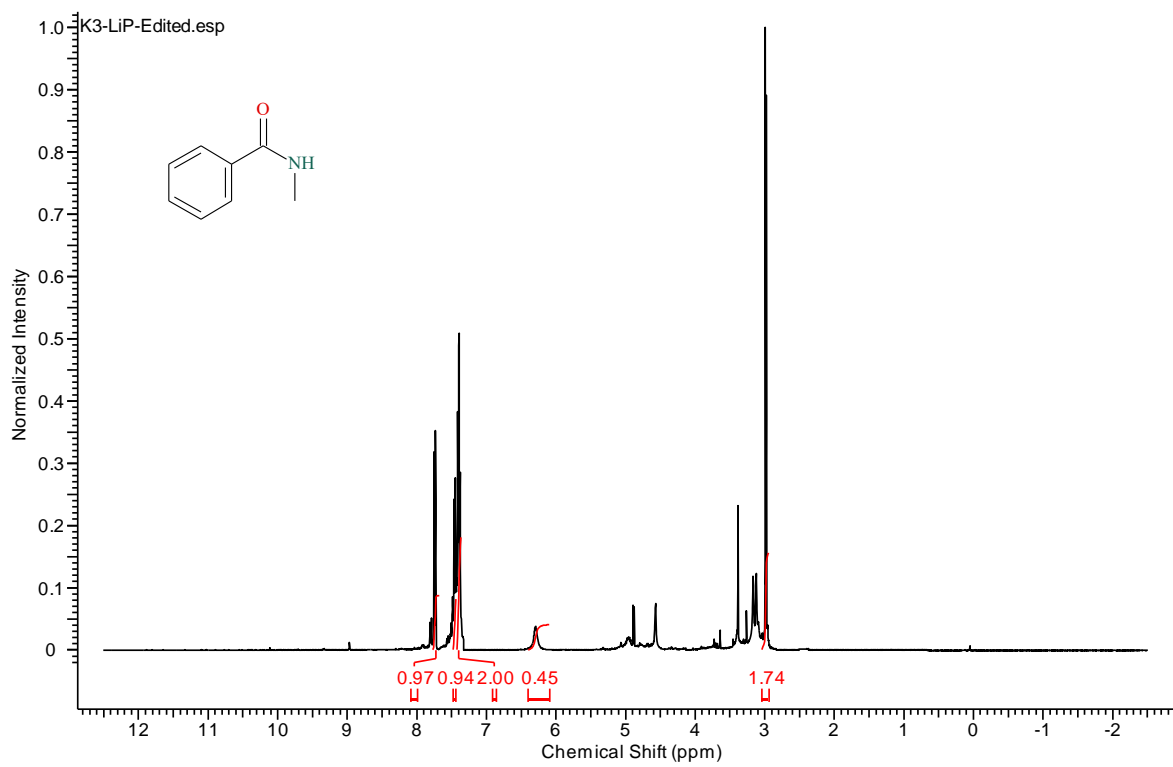
^{1}H-NMR spectra of **13** (400MHz, CDCl$_3$)